November 26th, 2019

To the Editors of *PLOS Pathogens*

Dear Editors,

Please find enclosed the manuscript entitled "Differential gene expression elicited by ZIKV infection in trophoblasts from congenital Zika syndrome discordant twins", by Amaral *et al*., which we are submitting to *PLOS Pathogens* as a research article. In this manuscript, we report for the first time the different susceptibilities to ZIKV *in vitro* infection of human-induced-pluripotent-stem-cell-derived (hiPSC-derived) trophoblasts from three pairs of twins discordant for congenital Zika syndrome (CZS).

Discordant twins represent a good case–control group to test for the genetic contribution determining the fetuses' outcome of gestational infection. Each of the twins' expectant mother has been infected during pregnancy, the two fetuses have been exposed to ZIKV at the same time during their embryonic development, and yet only one of them presented a CZS phenotype. To the best of our knowledge, no other study has compared the *in vitro* trophoblast gene expression profile or outcome of ZIKV infection in hiPSC-derived trophoblasts from discordant twins for CZS under the same experimental conditions.

We have previously shown that, in these three pairs of dizygotic twins discordant for CZS, the neural progenitor cells (NPCs) from the CZS-affected twins presented higher *in vitro* ZIKV susceptibility compared with NPCs from the non-affected (Caires-Junior *et al*., *Nat Commun* 9: 475, 2018). Here, we show that trophoblasts from CZS-affected twins were also significantly more susceptible to ZIKV infection when compared with trophoblasts from the non-affected. In addition, ZIKV infection caused, only in the trophoblasts from CZS-affected twins, the downregulation of genes related to extracellular matrix organization and to leukocyte activation, which are important for trophoblast adhesion and immune response activation. Notably, only trophoblasts from non-affected twins secreted significantly increased amounts of chemokines RANTES/CCL5 and IP10 after infection with ZIKV.

Taken together, these results show that development of congenital Zika syndrome might result among other factors from a concomitant decreased ability of the placenta to respond to ZIKV infection in the CZS-affected neonates, along with a deregulation of neural development genes in ZIKV-infected NPCs of these CZS-affected neonates. We are positive that this report will be of great interest to the readers of *PLOS Pathogens* and to those working in the field.

We would like to suggest one of the following editors to handle our submission: Michael S. Diamond or Ana Fernandez-Sesma.

We are looking forward to hearing from you.

Yours sincerely,

Sergio Verjovski-Almeida, MD, PhD
Laboratory of Gene Expression in Eukaryotes
Instituto Butantan
Av. Vital Brasil, 1500
05503-900 Sao Paulo, SP, Brazil
TEL +55 11 2627-3855
e-mail address: sergio.verjovski@butantan.gov.br

Differential gene expression elicited by ZIKV infection in trophoblasts from congenital Zika syndrome discordant twins

Murilo Sena Amaral[1¶], Ernesto Goulart[2¶], Luiz Carlos Caires-Júnior[2¶], David Abraham Morales-Vicente[1,3], Alessandra Soares-Schanoski[4], Roselane Paiva Gomes[5], Giovanna Gonçalves de Oliveira Olberg[1], Renato Mancini Astray[5], Jorge E. Kalil[6], Mayana Zatz[2], Sergio Verjovski-Almeida[1,3*]

[1]Laboratório de Parasitologia, Instituto Butantan, São Paulo, Brazil

[2]Departmento de Genética e Biologia Evolutiva, Centro de Pesquisas sobre o Genoma Humano e Células Tronco, Instituto de Biociências, Universidade de São Paulo, São Paulo, Brazil

[3]Departamento de Bioquímica, Instituto de Química, Universidade de São Paulo, São Paulo, Brazil

[4]Laboratorio de Bacteriologia, Instituto Butantan, São Paulo, Brazil

[5]Laboratorio de Imunologia Viral, Instituto Butantan, São Paulo, Brazil

[6]Laboratório de Imunologia, Faculdade de Medicina e Instituto do Coração, Universidade de São Paulo, São Paulo, Brazil

* Corresponding author:
Email: verjo@iq.usp.br (SVA)

¶These authors contributed equally to this work.

Short title: Molecular signatures from ZIKV-infected discordant twins' trophoblasts

Abstract

Zika virus (ZIKV) causes congenital Zika syndrome (CZS), which is characterized by fetal demise, microcephaly and other abnormalities. ZIKV in the pregnant woman circulation must cross the placental barrier that includes fetal endothelial cells and trophoblasts, in order to reach the fetus. CZS occurs in ~1-40% of cases of pregnant women infected by ZIKV, suggesting that mothers' infection by ZIKV during pregnancy is not deterministic for CZS phenotype in the fetus. Therefore, other susceptibility factors might be involved, including the host genetic background. We have previously shown that in three pairs of dizygotic twins discordant for CZS, neural progenitor cells (NPCs) from the CZS-affected twins presented differential *in vitro* ZIKV susceptibility compared with NPCs from the non-affected. Here, we analyzed human-induced-pluripotent-stem-cell-derived (hiPSC-derived) trophoblasts from these twins and compared by RNA-Seq the trophoblasts from CZS-affected and non-affected twins. Following *in vitro* exposure to a Brazilian ZIKV strain ($ZIKV^{BR}$), trophoblasts from CZS-affected twins were significantly more susceptible to $ZIKV^{BR}$ infection when compared with trophoblasts from the non-affected. Transcriptome profiling revealed no differences in gene expression levels of ZIKV candidate attachment factors, IFN receptors and IFN in the trophoblasts, either before or after $ZIKV^{BR}$ infection. Most importantly, $ZIKV^{BR}$ infection caused, only in the trophoblasts from CZS-affected twins, the downregulation of genes related to extracellular matrix organization and to leukocyte activation, which are important for trophoblast adhesion and immune response activation. In addition, only trophoblasts from non-affected twins secreted significantly increased amounts of chemokines RANTES/CCL5 and IP10 after infection with $ZIKV^{BR}$. Overall, our results showed that trophoblasts from non-affected twins have the ability to more efficiently activate genes that are known to play important roles in cell adhesion and in triggering the immune response to ZIKV infection in the placenta, and this may contribute to predict protection from ZIKV dissemination into fetuses' tissues.

53 ## Author summary

54 The Zika virus (ZIKV) infection in adults is usually characterized by mild flu-like symptoms,
55 with most cases remaining asymptomatic. However, in the last years, widespread ZIKV infection was
56 shown for the first time to be associated with congenital Zika syndrome (CZS) and death of neonates.
57 CZS is a very debilitating condition that includes microcephaly and mental retardation, leading to a
58 strong social and health impact. This dramatic condition calls for a careful evaluation of the
59 molecular mechanisms involved in ZIKV infection in the maternal-fetal interface. It is estimated that
60 CZS occurs in ~1-40% of cases of pregnant women infected by ZIKV, which suggests that different
61 susceptibility factors might be involved, including the host genetic background. By analyzing
62 trophoblast cells that recapitulate the placenta from three pairs of dizygotic twins discordant for CZS,
63 we were able to show that trophoblasts from CZS-affected twins were significantly more susceptible
64 to ZIKV infection when compared with trophoblasts from the non-affected twins. We also provide a
65 detailed picture of genes differentially expressed by trophoblasts from the discordant twins after
66 infection with ZIKV. These genes can be further investigated as possible therapeutic targets to avoid
67 viral dissemination into developing fetus' tissues.

68

69 ## Introduction

70 Zika virus (ZIKV) is a flavivirus with sporadic outbreaks reported in several countries,
71 causing an infection usually characterized by mild symptoms, where up to 80% of cases remain
72 asymptomatic [1-3]. However, most likely due to the mutation acquired during the large outbreak
73 recorded in French Polynesia in 2013–2014 [4-6], for the first time, widespread ZIKV infection was
74 shown to be associated with congenital Zika syndrome (CZS) and death of neonates [3,7-13].
75 CZS is characterized by variable clinical presentations, including fetal demise, microcephaly
76 and other abnormalities (hearing and ocular loss, mental retardation, epilepsy, muscle weakness,

77 learning disabilities and behavioral abnormalities) [14-16]. It is well established now that ZIKV
78 shows tropism for a wide range of host tissues [17-19], especially neuronal cell types, including
79 neural progenitor cells, mature neurons and astrocytes (reviewed by Christian et al. [20]), and
80 replicates in *ex vivo* slices from adult human cortical tissues [21]. Also, Zika virus infection
81 reprograms global transcription in the host cells [22]. ZIKV in the maternal circulation needs to cross
82 the placental barrier that includes fetal endothelial cells and trophoblasts in order to reach the fetus
83 [23,24]. Several placenta related cells have been shown to be infected by ZIKV, including placental
84 macrophages and trophoblasts [25-29].

85 It has been estimated that CZS occurs in ~1-40% of cases of pregnant women infected by
86 ZIKV [3,13,30,31]. This suggests that mothers' infection by ZIKV during pregnancy is not the only
87 factor determining CZS phenotype in the fetus, and other susceptibility factors might be involved.
88 Indeed, neural progenitor cells (NPCs) from different individuals have been shown to respond
89 differently to ZIKV infection [32,33]. In this scenario, discordant twins represent a good case–control
90 sample to test for the genetic contribution determining the fetuses' discordant outcome of gestational
91 infection with ZIKV, as they are supposed to have been exposed to ZIKV under similar conditions in
92 the uterus during gestation.

93 We have previously shown that twins discordant for CZS outcome show differential neural
94 progenitor cells (NPCs) *in vitro* viral susceptibility to a Brazilian ZIKV strain ($ZIKV^{BR}$) [32], but it
95 remains to be determined if discordant CZS twins also show differential placental susceptibility to
96 viral infection. Here, we compared the susceptibility and molecular signatures associated with *in*
97 *vitro* $ZIKV^{BR}$ infection of trophoblasts from the same CZS-affected and non-affected twins, using a
98 well-established trophoblasts model that recapitulates the primitive placenta formed during
99 implantation [34,35]. We show here that hiPSC-derived trophoblasts from CZS-affected twins were
100 significantly more susceptible to *in vitro* $ZIKV^{BR}$ infection when compared with trophoblasts from
101 non-affected twins. In this context, we had previously shown that, before infection, ESC-derived

102 trophoblasts express a wide range of attachment factors for ZIKV entry and lack the components of a
103 robust antiviral response system [35]; in contrast, cells from term placentas, which resist infection, do
104 not express genes encoding attachment factors implicated in ZIKV entry and do express many genes
105 associated with antiviral defense [35]. However, no ZIKV infection assays were performed with
106 these ESC-derived trophoblasts [35]. Here, transcriptome profiling of hiPSC-derived trophoblasts
107 revealed that ZIKV^{BR} infection elicited different responses in hiPSC-derived trophoblasts from CZS-
108 affected and non-affected twins, highlighting that genes involved with extracellular matrix
109 organization as well as with immune response activation in the placental tissue may contribute to
110 modulate ZIKV infection outcome.

111 Results

112 Infection with ZIKV^{BR} of hiPSC-derived trophoblasts from discordant twins

113 We obtained blood from three pairs of dizygotic twins discordant for CZS (non-affected:
114 #10608-4, #10763-4, and #10788-4; CZS-affected: #10608-1, #10763-1, and #10788-1) for
115 generation of hiPSC-derived trophoblasts and for phenotypic and gene expression analysis after *in*
116 *vitro* infection with ZIKV^{BR} (**Fig 1A**). Erythroblasts from the three pairs of DZ twins were
117 reprogrammed towards hiPSCs. All hiPSC lines were previously shown by immunofluorescence
118 staining to express markers of pluripotency (TRA-1-60 and OCT4) and by RT-qPCR to express
119 endogenous pluripotent transcription factors including *NANOG* and *OCT4* [32].
120 Then, the hiPSCs originated from the three pairs of twins were differentiated into primitive
121 trophoblasts using an established protocol [34,35] and further characterized to confirm their
122 differentiation *in vitro*. Under these conditions, we found that all hiPSC-derived trophoblast lines
123 robustly expressed chorionic gonadotropin subunit beta 3 (β-CG/ hCGB3) and keratin 7 (CK7/KRT7)
124 (**Fig 1B**), two of the most commonly used trophoblast markers [36].

125 Subsequently, we infected hiPSC-derived trophoblasts with ZIKV^{BR} using multiplicity of
126 infection (MOI) of 0.3 and 3, and at 96 hpi (hours post-infection) we investigated the viral titer by
127 measuring the number of plaque-forming units (PFU) in cell culture supernatants (**Fig 1C**). Virus
128 titers were significantly higher (2.8-fold) in the supernatant of CZS-affected twins' trophoblasts
129 infected with MOI 0.3 (**Fig 1C** and **1D**), indicating that trophoblasts from CZS-affected twins were
130 significantly more susceptible to ZIKV infection or at least more virus productive when compared
131 with trophoblasts from non-affected twins. Infection with the higher MOI (MOI = 3) obliterated this
132 difference due to the high susceptibility of trophoblasts in general to the Zika infection. In order to
133 have a better resolution of the differences between cells derived from CZS-affected and non-affected
134 twins, subsequent studies were performed with MOI of 0.3.

135 **Potential flavivirus attachment factors and IFN receptor genes were not differentially**
136 **expressed between trophoblasts from discordant twins**

137 To evaluate the possible differences in molecular signatures associated with ZIKV^{BR} infection
138 in trophoblasts from CZS-affected and non-affected twins, we performed RNA-Seq analysis in
139 hiPSC-derived trophoblasts before and after *in vitro* infection with ZIKV^{BR} for 96 h (MOI = 0.3).
140 With this approach, we could analyze possible differences in gene expression of potential attachment
141 factors for ZIKV and of genes related to antiviral response.

142 We first confirmed the efficiency of hiPSC differentiation into trophoblasts by looking at the
143 expression levels of a set of over100 genes which have been associated with the trophoblast lineage
144 of mammals [35,36]. When compared with hiPSCs, most of these genes showed significant
145 upregulation in trophoblasts after differentiation (**S1 Table**). We validated by RT-qPCR the
146 differential expression of *NANOG*, a hiPSC marker, and of *HCGA*, *HCGB* and *KRT7*, three of the
147 genes upregulated in the trophoblasts upon differentiation, as compared with the hiPSCs (**S1 Fig**).
148 Consistent with this and with previous experiments that used the same differentiation protocol [35],

149 proliferation-related genes were downregulated in the trophoblasts relative to the hiPSCs (**S2 Fig**). In
150 addition, four genes encoding transcription factors – *CDX2, ELF5, EOMES* and *ASCL1,* which are
151 generally regarded as markers of trophoblast stem cells [37] – were found to be barely expressed
152 (TPM < 1) in all six hiPSC-derived trophoblast samples from the twins analyzed here. This suggests
153 that all trophoblasts from all the twins differentiated beyond the trophoblast stem-cell stage.

154 We then looked for differences in the expression levels of potential flavivirus attachment
155 factor genes, of IFN genes and of IFN receptor genes between the trophoblasts from CZS-affected
156 and non-affected twins. These differences could be related to the greater susceptibility to $ZIKV^{BR}$
157 infection of the trophoblasts from CZS-affected twins.

158 Many potential flavivirus attachment factors have been proposed as ZIKV candidate
159 receptors, including glycosaminoglycans (CD209/DC-SIGN and HSPG*2*) and TAM receptors
160 (TYRO3, AXL, MERTK) [38-40]. None of these receptor genes was found to be differentially
161 expressed between the trophoblasts from CZS-affected and non-affected twins (**S3 Fig**). *CD209/DC-*
162 *SIGN* gene was barely expressed in the hiPSC-derived trophoblasts either before or after $ZIKV^{BR}$
163 infection (**S3 Fig**). *HSPG2* gene had the highest expression levels in hiPSC-derived trophoblasts
164 among the genes encoding potential ZIKV candidate receptors, however no differences in the
165 expression levels of *HSPG2* gene between trophoblasts from CZS-affected and non-affected twins
166 were found either before or after $ZIKV^{BR}$ infection (**S3 Fig**). Recently, AXL has been reported as the
167 receptor involved in ZIKV entry in many cell types, including neural stem cells [41], human
168 umbilical vein endothelial cells (HUVECs) [42], primary human astrocytes [43] and Sertoli cells
169 [44]. *AXL* gene expression showed a marked increase upon differentiation from hiPSC towards
170 trophoblasts (> 5-fold on average), but infected and non-infected hiPSC-derived trophoblasts from
171 non-affected or CZS-affected twins show similar expression levels of *AXL* gene (**S3 Fig**). TAM-
172 family receptors bind phosphatidylserine indirectly, through the soluble intermediates GAS6 (growth
173 arrest-specific 6) and PROS1 [45]. Recently, it was shown that ZIKV infects HUVECs much more

174 efficiently than other flaviviruses because it binds GAS6 more avidly, which in turn facilitates its
175 interaction with AXL [42]. Infected and non-infected hiPSC-derived trophoblasts from non-affected
176 or CZS-affected twins show similar expression levels of *GAS6* and *PROS1* genes (**S3 Fig**). HAVCR1
177 (TIM1; hepatitis C receptor) was shown to have an important role in the entry of ZIKV into primary
178 cell types from mid- and late-gestation placentas and explants from first-trimester chorionic villi
179 [26]. Interestingly, *HAVCR1* gene was barely expressed in all the hiPSC-derived trophoblasts (**S3**
180 **Fig**). Expression levels of all the above receptor genes measured here in non-infected hiPSC-derived
181 trophoblasts from the three pairs of twins confirmed previous data from ESC-derived non-infected
182 trophoblasts [35].

183 Production of interferons has been reported as a key step in the antiviral immune response to
184 ZIKV [25,46,47]. In agreement with Sheridan et al. [35], primitive trophoblasts expressed low levels
185 of mRNAs from all the IFN genes (**S4 Fig**) when compared with ZIKV potential attachment factors
186 (**S3 Fig**). Upon *in vitro* infection with $ZIKV^{BR}$, a marked induction of mRNA expression of *IFNB1*,
187 *IFNL1*, *IFNL2* and *IFNL3* genes but not of *IFNE* was observed (**S4 Fig**). Of note, IFN genes were
188 not differentially expressed between the trophoblasts from CZS-affected and non-affected twins (**S4**
189 **Fig**). *IFNA*, *IFNG, IFNK* and *IFNW1* genes were not detectable in any hiPSC-derived trophoblast
190 cells.

191 Interestingly, *IFNGR1* and *IFNGR2* (type II IFN receptor genes) were highly upregulated in
192 hiPSC-derived trophoblasts when compared with the hiPSCs that originated them (**S5 Fig**). These
193 two IFN receptor genes were not differentially expressed between trophoblasts from CZS-affected
194 and non-affected twins, and their expression was not changed upon $ZIKV^{BR}$ infection (**S5 Fig**).
195 Compared with the expression of type II IFNR genes, the expression levels of the other interferon
196 receptor genes, namely type I IFNR (*IFNAR1* and *IFNAR2*) and the first (*IFNLR1*) and second

197 (*IL10RB*) subunits of type III IFNR gene (*IFNL*) were lower in both hiPSCs and hiPSC-derived
198 trophoblasts (**S5 Fig**), and again none of them had their expression affected by ZIKV^{BR}.

199 **Induction of interferon-stimulated genes (ISGs) expression and of IFN secretion in hiPSC-**
200 **derived trophoblasts upon ZIKV^{BR} infection**

201 It is known that interferons participate as mediators of the response to ZIKV infection in the
202 maternal-fetal interface [25,48,49] and that ESC-derived trophoblasts lack components of a robust
203 antiviral response system before infection with ZIKV [35]. However, it is not known if hiPSC-
204 derived primitive trophoblasts are able to induce an antiviral response after infection with ZIKV. To
205 determine this, we analyzed our RNA-Seq data and looked for differentially expressed genes (DEGs)
206 in the hiPSC-derived primitive trophoblasts after *in vitro* infection with ZIKV^{BR}.
207 An important gene expression response was induced in both hiPSC-derived trophoblasts from
208 CZS-affected and non-affected twins following *in vitro* infection with ZIKV^{BR}, and a set of 471
209 DEGs were upregulated in hiPSC-derived trophoblasts after infection with ZIKV^{BR} (FDR < 0.05,
210 Edge R exact test) (**Fig 2A**). These genes (**S2 Table**) include interferon-stimulated genes (ISG) and
211 genes related to cytokine secretion. We found a significant (FDR < 0.05, cumulative hypergeometric
212 distribution) enrichment of different Gene Ontology (GO) terms among these 471 upregulated DEGs
213 detected in the RNA-Seq experiment, being the top categories "response to type I interferon",
214 "defense response to virus" and "negative regulation of viral process" (**Fig 2B, S3 Table**). Consistent
215 with the GO analysis, Ingenuity Pathway Analysis (IPA) also pointed to an enriched network of
216 interferon-stimulated genes upregulated in hiPSC-derived trophoblasts after ZIKV infection
217 (upregulated ISGs are colored in pink in **Fig 3A**).
218 We also quantified in the hiPSC-derived trophoblasts the secreted levels of type I (IFNA2),
219 type II (IFNG) and type III (IFNL1) IFNs produced by these cells in the absence of virus or after
220 infection with ZIKV^{BR} and culture for 48 h (**Fig 3B, upper panel**) or 96 h (**Fig 3B, lower panel**).

221 After 48 h in culture without infection, hiPSC-derived trophoblasts from both CZS-affected and non-
222 affected twins were able to secrete IFNA2 and IFNG, whereas IFNL1 was not detectable. There was
223 no statistically significant increase in any IFN secretion at 48 h after $ZIKV^{BR}$ infection of
224 trophoblasts (**Fig 3B, upper panel**). After 96 h in culture, hiPSC-derived trophoblasts from both
225 CZS-affected and non-affected twins secreted higher levels of IFNA2, IFNG and IFNL1 compared
226 with those at 48 h, although high variability in the secreted IFN levels was observed among the
227 trophoblasts from different individuals (**Fig 3B, lower panel**). More importantly, a statistically
228 significant increase in the secretion of IFNL1 by trophoblasts from non-affected twins was observed
229 at 96 h after infection with $ZIKV^{BR}$, but not by trophoblasts from CZS-affected twins (**Fig 3B, lower**
230 **panel**).

231 Taken together, these results indicate that hiPSC-derived trophoblasts from both CZS-
232 affected and non-affected twins were able to respond to $ZIKV^{BR}$ infection by secreting IFNA2, IFNG
233 and IFNL1, which induced the upregulation of a set of ISG genes potentially involved in the response
234 to $ZIKV^{BR}$ infection. In addition, only trophoblasts from non-affected twins showed a significant
235 increase in secreted IFNL1 at 96 hpi with $ZIKV^{BR}$ (**Fig 3B, lower panel**).

236 **A set of genes involved with extracellular matrix organization and leukocyte activation was**
237 **downregulated in trophoblasts from CZS-affected twins after $ZIKV^{BR}$ infection**

238 We next investigated if there were differences in gene expression between trophoblasts from
239 CZS-affected and non-affected twins after $ZIKV^{BR}$ infection. In total, 44 genes were downregulated
240 after $ZIKV^{BR}$ infection in trophoblasts from CZS-affected when compared with non-affected twins
241 (FDR < 0.05, Edge R exact test) (**Fig 4A and S4 Table**). Different Gene Ontology (GO) terms were
242 found to be significantly (FDR < 0.05, cumulative hypergeometric distribution) enriched among
243 these 44 downregulated DEGs, including "extracellular matrix" and "regulation of leukocyte
244 activation" (**Fig 4B, S5 Table**). Significantly enriched Gene Ontology (GO) terms that were found

245 among the upregulated DEGs are shown in **S6 Fig** and **S5 Table**, and the most significantly enriched
246 categories are "amino acid biosynthetic process" and "acid secretion".

247 The levels of a panel of cytokines and chemokines secreted by the hiPSC-derived
248 trophoblasts were quantified in the supernatants of 48 h or 96 h cell cultures in the absence of virus
249 or after infection with $ZIKV^{BR}$. Interestingly, from all the analytes tested, the chemokines
250 RANTES/CCL5 and IP10 showed a consistent (both at 48 h and 96 h post-infection) and significant
251 increase in secretion by trophoblasts from non-affected twins after infection with $ZIKV^{BR}$, but not by
252 trophoblasts from CZS-affected twins (**Fig 4C**). RANTES/CCL5 secretion levels by trophoblasts
253 from non-affected twins increased 2.4- and 4.6-fold at 48 h or 96 h after infection with $ZIKV^{BR}$,
254 respectively, while IP10 secretion levels increased 16- and 96-fold (**Fig 4C**). The other tested
255 cytokines and chemokines did not show statistically significant differences in the levels produced by
256 infected trophoblasts from CZS-affected or non-affected twins.

257 Discussion

258 Here, we were able to analyze, for the first time, the *in vitro* viral susceptibility and the gene
259 expression patterns after *in vitro* $ZIKV^{BR}$ infection of hiPSC-induced trophoblasts from dizygotic
260 (DZ) twins discordant for the presence of microcephaly. Because these are DZ twins whose mothers
261 were infected with $ZIKV^{BR}$ during pregnancy, the two fetuses in each of the three twin pairs were
262 exposed to the virus at the same time, thus representing a rare and unique cohort to test whether the
263 host genetic background plays any role in determining CZS outcome. Indeed, we have previously
264 shown that hiPSC-induced NPCs from the same subjects exhibit differential *in vitro* $ZIKV^{BR}$
265 susceptibility, as NPCs from CZS-affected twins had significantly higher $ZIKV^{BR}$ replication and
266 reduced cell growth when compared with NPCs from non-affected twins [32]. No rare Mendelic
267 potentially pathogenic variant was assigned in this cohort that could explain NPCs susceptibility to
268 CZS [32], suggesting that CZS caused by ZIKV may be a multifactorial disorder. Herein, using a

269 well-established model that recapitulates the primitive placenta formed during fetal implantation
270 [34,35], we sought to investigate if hiPSC-induced trophoblasts from the same twins also show
271 differential responses to *in vitro* ZIKV^{BR} infection.

272 Many studies have established causal effects between ZIKV infection during pregnancy and
273 microcephaly developed in the fetus [15], using *in vitro* as well as mice and non-human primates *in*
274 *vivo* models [50-54]. Cells localized in the epidermis and dermis were primarily considered as
275 targets for ZIKV infection [55], as mosquito bite remains the major transmission route [56]. ZIKV
276 infection exhibits broad distribution and persistence in body tissues and fluids, and the presence of
277 ZIKV in the amniotic fluid of pregnant women and in semen [57-61] suggests the additional
278 possibility of sexual and perinatal transmissions. Trophectoderm cells of pre-implantation human
279 embryos can be infected with ZIKV [62]. Also, endometrial stromal cells are highly permissive to
280 ZIKV infection, and likely represent a crucial cell target of ZIKV reaching them, either via the
281 uterine vasculature in the viremic phase of the infection or by sexual viral transmission, being a
282 potential source of virus spreading to placental trophoblasts during pregnancy [63]. Indeed, recent
283 studies suggest that the placenta is the key mediator for vertical transmission of ZIKV from infected
284 mothers to fetal brains; several placental cells have been shown to be infected by ZIKV, including
285 placental macrophages, trophoblasts and fibroblasts of the maternal *decidua basalis* [25-29,35,58].
286 Here, we show that hiPSC-induced trophoblasts from DZ twins discordant for CZS were
287 differentially susceptible to infection with ZIKV^{BR}. Interestingly, 96 hpi with ZIKV^{BR}, virus titers in
288 culture supernatants were significantly higher in the CZS-affected twins' trophoblasts when
289 compared with non-affected (**Fig 1C**), indicating that ZIKV^{BR} can replicate more efficiently in the
290 trophoblasts from CZS-affected twins, potentially facilitating virus dissemination into fetal tissues.

291 Noteworthy, our RNA-seq results indicate that hiPSC-derived trophoblasts express the ZIKV
292 candidate receptor genes (*HSPG2* and *TAM* receptor genes) and the IFN receptor genes, and at lower

293 levels the IFN genes; however none of these genes were differentially expressed between the
294 trophoblasts from CZS-affected and non-affected twins either before or after ZIKV^{BR} infection.
295 Interestingly, ZIKV^{BR} infection caused a significant increase in IFNL1 secretion by
296 trophoblasts from non-affected twins (**Fig 3B**), whereas in trophoblasts from CZS-affected twins no
297 significant increase was observed (**Fig 3B**). IFNL1 is a type III IFN constitutively released by
298 primary human trophoblasts from full-term placentas [25], which are known to be refractory to ZIKV
299 infection [25,35]. The increased secretion of IFNL1 by trophoblasts from non-affected twins, already
300 at 48 hpi by ZIKV^{BR}, but especially at 96 hpi, may protect against ZIKV^{BR} dissemination, as shown
301 in the female reproductive tract of mice [47,64,65]. Our results indicate a possible role of IFNL1 in
302 the control of ZIKV infection by primitive trophoblasts. In addition, after ZIKV^{BR} infection,
303 trophoblasts from the non-affected twins were able to significantly induce the secretion of immune
304 mediator chemokines RANTES/CCL5 [66,67] and IP10 [68], while trophoblasts from the CZS-
305 affected twins were not (**Fig 4C**). RANTES/CCL5 promotes trophoblasts cell migration and can
306 recruit immune cells [69-71], whereas IP10 plays a role as a chemotactic molecule implicated in the
307 migration of trophoblast cells [72]. Thus, lower secretion of RANTES/CCL5 and IP10 indicates that
308 CZS-affected twins' trophoblasts have a lower ability of migration, immune cell recruitment and
309 viral control.
310 The placenta plays a critical role in immunological protection and can undergo major
311 structural and functional adaptations in order to protect the fetus from environmental stressors
312 [48,49]. When the placental function is impaired [73], the intrauterine environment might be
313 perturbed and the placental defenses involved in fetal protection compromised. In the RNA-Seq
314 analysis, we found 79 differentially expressed genes in common among the three CZS-affected
315 compared with non-affected twins, 44 of which were downregulated after ZIKV^{BR} infection in the
316 trophoblasts from CZS-affected compared with non-affected twins. The top GO category associated
317 with these downregulated differentially expressed genes is "extracellular matrix". It is known that for

318 successful fetus development, one of the critical steps is proper invasion of the maternal decidua by
319 trophoblasts [74] and that many molecules, including galectins, are involved in this process [75,76].
320 One of the downregulated genes in the trophoblasts from CZS-affected twins after ZIKV^{BR}
321 infection was *COL3A1* (**Fig 4A**). Collagens are the main structural proteins in the extracellular
322 matrix, and they have been related to pregnancy and/or placental pathological conditions including
323 gestational diabetes and pre-eclampsia [77,78]. *ITGA1*, another gene downregulated in trophoblasts
324 from CZS-affected twins after ZIKV^{BR} infection, interacts with the extracellular matrix, particularly
325 with collagen and laminin [79]. Importantly, extravillous trophoblasts (EVT) have been shown to
326 express ITGA1 as they invade from the anchoring villi deeply into the maternal endometrium and
327 myometrium in weeks 8–13 of gestation [80,81]. EVTs fail to express ITGA1 in preeclampsia, which
328 is associated with both poor trophoblast invasion and oxidative stress [81,82]. In addition, *LGALS3*
329 gene (encoding galectin-3) was downregulated in trophoblasts from CZS-affected twins after ZIKV^{BR}
330 infection. LGALS3 is a galectin that has been described as involved in the process of trophoblast cell
331 migration and invasion, significant for human embryo implantation [83,84]. Overall, downregulation
332 of genes involved in trophoblast adaptation to the intrauterine environment, including *ITGA1,*
333 *COL3A1* and *LGALS3* (**S7 Fig**), in the trophoblasts of CZS-affected twins after ZIKV^{BR} infection,
334 may affect trophoblast migration, implantation, homeostasis and possibly impair the control of
335 ZIKV^{BR} infection. Noteworthy, all the above differentially expressed genes were found in common
336 among the three CZS-affected compared with non-affected twins, in spite of the genetic background
337 variability of our cohort. Importantly, as all experiments were done under the same conditions, these
338 differences in genetic background underlie both possible differences in progression of trophoblasts
339 differentiation and the resulting difference in susceptibility to ZIKV infection. Thus, the set of 79
340 differentially expressed genes found here represents the minimum core of genes significantly altered
341 in common among the three pairs of twins. This study provides genetic targets to be further explored
342 as possible infection susceptibility factors in the placenta.

343 Our gene expression results indicate that ZIKV^{BR} infection has caused, only in the
344 trophoblasts from CZS-affected twins, the downregulation of genes important for trophoblast
345 adhesion as well as immune response activation. Noteworthy, when gene expression differences
346 between the NPCs from these non-affected and CZS-affected twins were analyzed [32], another set
347 of 64 genes was found to be differentially expressed, including *FOXG1* and *LHX2*, two transcription
348 factors important for neural development [85,86], which were down-regulated in NPCs from CZS-
349 affected compared with non-affected twins [32]. Overall, development of congenital Zika syndrome
350 might result, among other factors, from a concomitant decreased ability of the placenta to respond to
351 ZIKV infection in the CZS-affected neonates, along with a deregulation of neural development genes
352 in ZIKV-infected NPCs of these CZS-affected neonates.
353 Based on our gene expression analyses, we suggest that the ability to respond more efficiently
354 to ZIKV infection in the placenta may be a key parameter to predict the success of ZIKV
355 dissemination into fetuses' tissues. Moreover, further understanding of the participation of immune
356 mediators, such as the chemokines RANTES/CCL5 and IP10, in the trophoblast response to ZIKV
357 infection may open a path for drug development or repurposing to possibly inhibit viral replication or
358 avoid viral dissemination into fetus' tissues.
359

360 ## Materials and methods

361 ### Human subjects

362 Three pairs of DZ-D (dichorionic and diamniotic) twins discordant for the presence of
363 microcephaly (#10608-1 and #10608-4; #10763-1 and #10763-4; #10788-1 and #10788-4) whose
364 peripheral blood mononuclear cells had been previously collected and isolated [32] were examined in
365 this study. Zygosity had been previously confirmed by whole-exome sequencing (WES) and by

366 microsatellite analysis [32]. All babies were born from mothers negative for previous STORCH
367 infections and in each affected baby (#10608-1, #10763-1 and #10788-1) the head circumference was
368 three standard deviations (SD) below the mean for the given age, sex, and gestation stage at birth
369 [32,87]. Diagnosis of microcephaly due to ZIKV infection (CZS) in all the three affected subjects
370 was confirmed by neuroimaging, serology and by the mother reporting ZIKV infection symptoms
371 during pregnancy (**S6 Table** and Caires-Junior et al. [32]). The protocol used in this study was
372 approved by the Human Research Ethics Committee from Biosciences Institute, University of São
373 Paulo (protocol # 184/2016). All mothers gave written informed consent in accordance with the
374 Declaration of Helsinki.

375 **Cell lines and maintenance of hiPSCs**

376 hiPSCs were generated according to Caires-Junior et al. [32]. Briefly, CD71+ cells were
377 isolated from the three pairs of DZ-D twins' peripheral blood samples (#10608-1 and #10608-4;
378 #10763-1 and #10763-4; #10788-1 and #10788-4). CD71-positive cells were sorted using magnetic
379 labeled antibody (Miltenyi) following the manufacturer's instructions. All hiPSC lines were tested
380 for ZIKV infection by RT-qPCR using primers described in **S7 Table** and the results were negative.
381 The reprogramming protocol was performed with episomal vectors system (Addgene plasmids
382 27077, 27078 and 27080), and using the Amaxa human CD34+ cells Nucleofection Kit (Lonza),
383 following the manufacturer's recommendations. Three days after nucleoporation, cells were seeded
384 on irradiated murine embryonic fibroblasts (Millipore, A24903) in embryonic stem cell (ESC)
385 medium (Dulbecco's modified Eagle's medium (DMEM)/F12 supplemented with 2 mM GlutaMAX-
386 I, 0.1 mM non-essential amino acids, 100 μM 2-mercaptoethanol, 20% knockout serum replacement
387 (all provided by Life Technologies), 10 ng/mL bFGF (Peprotech), 0.25 mM NaB, 0.5 mM VPA, 2
388 μM thiazovivin, 0.5 μM PD 0325901 and 2 μM SB 431542; all provided by Tocris Bioscience). The
389 typical hiPSC colonies were transferred to hESC-qualified Matrigel (Corning)-coated 60 mm petri

390 dishes (Corning) and cultured in Essential 8 Medium (Gibco) with 100 µg/mL normocin
391 (InvivoGen). All derived cell lines were checked for mycoplasma contamination periodically.

392 **Differentiation of human iPSCs into trophoblasts**

393 Differentiation of human iPSCs into trophoblasts was performed according to Amita et al.
394 [34]. Briefly, hiPSCs were seeded at 15,000 cells/cm^2 on Matrigel (Corning) coated plates and
395 cultured in mTESR1 medium (Stem Cell Technologies) for 3 days with daily medium changes. Next,
396 basal medium was changed to hES medium supplemented with 4 ng/mL FGF-2 for 24 h. For the next
397 9 days, hES-BAP medium was used, which consisted of hES medium supplemented with BMP4 (10
398 ng/mL), A83-01 (1 µM) and PD173074 (0.1 µM), with daily medium changes. hES medium was
399 composed of DMEM/F-12 supplemented with 20 % KO-serum replacement, 1 % NEAA, 1 %
400 glutamine, 0.1 mM 2-mercaptoethanol, all from Gibco.

401 **In situ immunofluorescence**

402 hiPSCs and trophoblast cultures were fixed with 4 % PFA followed by permeabilization with
403 0.01 % Triton X-100 and then blocked with 5 % bovine serum albumin (BSA) for 1 h. The cells were
404 incubated overnight with primary antibodies at 4 °C (Anti-hCG beta/β-CG/hCGB3, Abcam #ab53087
405 and Anti-Cytokeratin 7/CK7/KRT7, Abcam #ab9021), washed with PBS and subsequently incubated
406 with secondary fluorescent antibodies for 1 h at room temperature. Finally, cells were stained with
407 DAPI (4',6-diamidino-2-phenylindole) and or Phalloidin for 2 min at room temperature. Confocal
408 analysis was performed using Zeiss LSM 800.

409 **Zika virus**

410 ZIKV^{BR} was a courtesy of Dr. Pedro Vasconcelos [88], Instituto Evandro Chagas, Brazil.
411 Viral stock was established after viral propagation for two serial passages in VERO cells (ATCC®
412 CCL-81™) in serum-free medium (VP SFM, Thermo scientific).

413 **Infection of the hiPSC-derived trophoblasts**

414 hiPSC-derived day-9 trophoblasts were seeded into 6-well or 24-well plates (Corning) and 2-
415 well chamber slides (Nunc; Thermo Fisher Scientific) to a confluence of 3×10^4 cells/cm^2.
416 Trophoblasts (monolayer) were exposed to ZIKV^{BR} (MOI: 0.3, 3 and Mock). Monolayer cells were
417 exposed to the virus for 1 h at 37 °C and 5 % CO_2 (g), washed with hES-BAP medium, and then
418 maintained by up to 96 h (end point).

419 **Measurement of viral burden**

420 For ZIKV titration, plaque assay was performed with the supernatants of cell cultures. For
421 plaque assay, an amount of 6×10^4 VERO cells/well were seeded in 24-well plates 48 h before the
422 assay. Samples were serially diluted in DMEM culture medium from 10^{-1} to 10^{-6}, applied in
423 duplicates of 100 µL to each well, and incubated for 30 min at 37 °C. After virus adsorption, wells
424 were overlaid with culture medium containing carboxymethyl cellulose (1 %) and incubated at 37 °C.
425 After 5 days, plates were drained, washed with PBS, and stained with 0.1 % naphthol blue-black, 1.6
426 % sodium acetate in 6 % glacial acetic acid for 30 min. Plaque formation units were visually
427 determined in the most appropriate viral dilution and expressed as PFU/mL.

428 **RNA-Seq assay**

429 Total RNA from hiPSC-derived trophoblasts was extracted using the RNeasy Micro Kit
430 (Qiagen, 74004), treated with TURBO DNase (Ambion, AM2238) for 30 min at 37 °C, and then re-
431 purified with the Qiagen RNeasy Micro Kit. RNA samples were quantified using the Qubit RNA HS

432 Assay Kit (Thermo Fisher Scientific, Q32852); purity was evaluated using NanoDrop ND-1000
433 Spectrophotometer (NanoDrop Technologies) and the integrity was verified using the Agilent RNA
434 6000 Pico Kit (Agilent Technologies, 5067-1513) in the 2100 Bioanalyzer Instrument (Agilent
435 Technologies). Stranded tagged cDNA libraries were prepared using the KAPA Stranded mRNA-Seq
436 Kit (Illumina, KK8421) and cluster generation was performed using the Illumina HiSeq 4000 PE
437 Cluster Kit (Illumina, PE-410-1001). Tagged libraries were pooled and sequenced (300 cycles,
438 paired-end sequencing) in the Illumina HiSeq 4000 instrument using a HiSeq 4000 SBS Kit
439 (Illumina, FC-410- 1003). Raw reads were preprocessed using the standard Illumina pipeline to
440 segregate multiplexed reads.

441 **RNA-seq data processing and analysis**

442 Paired-end adapters and low quality reads were removed by fastp version 0.20.0 [89] using
443 the quality-filtering parameters -l 20 -5 3 -3 3. Filtered paired-end reads were mapped and quantified
444 at gene level by the STAR-RSEM pipeline [90,91], using an index made from GRCh38.p12
445 GencodeV.28 [92]. All differential expression (DE) analyses used the bioconductor package edgeR
446 [93]. To call differentially expressed genes a general linear models (glm) was fitted, and likelihood
447 ratio tests (lrt) were performed using twins' covariates as blocking groups in all cases. P-values were
448 adjusted using FDR, all genes with FDR lower than 0.05 were considered differentially expressed
449 genes. To identify up-regulated or down-regulated genes, the logCPM data from edgeR were used.
450 Heatmaps were plotted using the R package pheatmap. Enriched gene ontology analysis was perform
451 using the bioconductor package clusterProfiler [94], based on the annotation of the bioconductor
452 package org.Hs.eg.db. All plots were generated with the R packages gg plot2, cowplot and the
453 bioconductor package DOSE.

454 **Reverse transcription - quantitative PCR (RT-qPCR)**

455 Total RNA from hiPSCs and hiPSC-derived trophoblasts was extracted as described above.
456 The reverse transcription (RT) reaction was performed with 150 ng of each total RNA sample using
457 the SuperScript IV First-Strand Synthesis System (Life Technologies, cat. #18091050) and random
458 hexamer primers in a 20 µL final volume. The obtained cDNAs were diluted 10 times in water and
459 quantitative PCR was performed using 2.5 µL of each diluted cDNA in a total volume of 10 µL
460 containing 1× LightCycler 480 SYBR Green I Master Mix (Roche Diagnostics, cat. #04707516001)
461 and 800 nM of each primer in a LightCycler 480 System (Roche Diagnostics). RT-qPCR was run in
462 two biological replicates with three technical replicates each and primers are shown in **S7 Table**. The
463 GAPDH gene (NM_002046) was used as the reference for internal normalization.

464 **Cytokine and chemokine protein quantification**

465 Supernatants from trophoblasts' cell cultures were collected after 48 h or 96 h of infection
466 with $ZIKV^{BR}$ and then evaluated for 33 cytokines/chemokines for the following analytes: IFNalfa2,
467 IFNbeta, IFNg, IFN-lambda1/ IL-29, IFN-lambda 2/ IL28a, IL6, IL10, IL12p40, IL12p70, IL13,
468 IL15, IL17A, IL1RA, IL1a, IL1b, IL2, IL3, IL4, IL5, IL7, IL8, IP10, MCP1, MIP1a, MIP1b,
469 RANTES, TNFa, TNFb, VEGF, EGF, EOTAXIN, GCSF and GMCSF. The Human
470 Cytokine/Chemokine Magnetic Bead Panel kit (Millipore) was used according to the manufacturer's
471 recommendations. Samples were analyzed in the MagPix instrument (Luminex) and the data was
472 analyzed with the Milliplex Analyst software (Millipore).

473 **Quantification and statistical analysis**

474 Two-tailed unpaired t test was used for pairwise comparisons. Graphpad Prism software was
475 used to perform statistical analysis (version 7.0). Quantification of data are represented as mean ±
476 SEM and p-value threshold was * 0.05, ** 0.01, *** 0.001 and **** 0.0001.
477

Data availability

The RNA-Seq data that support the findings of this study have been deposited in the Sequence Read Archive (SRA) NCBI repository under Accession number PRJNA565997. All other data supporting the findings of this study are available within the article and its Supporting Information files or are available from the authors upon request.

Acknowledgments

We thank Dr. R. Michael Roberts and Dr. Toshihiko Ezashi, University of Missouri, Columbia, MO, USA for advice on trophoblast cells cultivation protocols. We thank Dr. J.C. Setubal for access to the computational facilities of the Bioinformatics Laboratory of Instituto de Química, Universidade de São Paulo, São Paulo, Brazil.

Author contributions

Conceptualization: Murilo Sena Amaral, Sergio Verjovski-Almeida

Data Curation: Murilo Sena Amaral, David Abraham Morales-Vicente, Sergio Verjovski-Almeida

Formal Analysis: Murilo Sena Amaral, Ernesto Goulart, Luiz Carlos Caires-Júnior, Alessandra Soares-Schanoski, Jorge E. Kalil, Mayana Zatz, Sergio Verjovski-Almeida

Funding Acquisition: Mayana Zatz, Sergio Verjovski-Almeida

Investigation: Murilo Sena Amaral, Ernesto Goulart, Luiz Carlos Caires-Júnior, Alessandra Soares-Schanoski, Roselane Paiva Gomes, Giovanna Gonçalves de Oliveira Olberg

Methodology: Murilo Sena Amaral, Ernesto Goulart, Luiz Carlos Caires-Júnior, David Abraham Morales-Vicente, Alessandra Soares-Schanoski, Sergio Verjovski-Almeida

Project Administration: Mayana Zatz, Sergio Verjovski-Almeida

Resources: Renato Mancini Astray, Mayana Zatz, Sergio Verjovski-Almeida

Software: David Abraham Morales-Vicente

Supervision: Jorge E. Kalil, Mayana Zatz, Sergio Verjovski-Almeida

Validation: Murilo Sena Amaral, Ernesto Goulart, Luiz Carlos Caires-Júnior, David Abraham Morales-Vicente

Visualization: Murilo Sena Amaral, David Abraham Morales-Vicente

Writing – Original Draft Preparation: Murilo Sena Amaral, Sergio Verjovski-Almeida

Writing – Review & Editing: Murilo Sena Amaral, Ernesto Goulart, Luiz Carlos Caires-Júnior, Alessandra Soares-Schanoski, Renato Mancini Astray, Jorge E. Kalil, Mayana Zatz, Sergio Verjovski-Almeida

Competing interests

The authors have declared that no competing interests exist.

Financial disclosure statement

This work was supported by grants from Fundação de Amparo à Pesquisa do Estado de São Paulo (FAPESP) (Thematic grant number 2014/03620-2 and 2018/23693-5 to SVA and CEPID number 2013/08028-1 and INCT number 14/50931-3 to MZ) and from Conselho Nacional de Desenvolvimento Científico e Tecnológico (CNPq) INCT number 465355/2014-5 to MZ. DAMV received a fellowship from Coordenação de Aperfeiçoamento de Pessoal de Nível Superior (CAPES), Brazil – Finance Code 001; LCCJ is a fellow of FAPESP (2017/16283-2); EG is a fellow of FAPESP (2015/14821-1); SVA laboratory was also supported by institutional funds from Fundação Butantan; SVA received an established investigator fellowship award from CNPq, Brazil. The funders had no role in study design, data collection and analysis, decision to publish, or preparation of the manuscript.

522 **References**

523 1. Duffy MR, Chen TH, Hancock WT, Powers AM, Kool JL, et al. (2009) Zika virus outbreak on
524 Yap Island, Federated States of Micronesia. N Engl J Med 360: 2536-2543.

525 2. Cao-Lormeau VM, Roche C, Teissier A, Robin E, Berry AL, et al. (2014) Zika virus, French
526 polynesia, South pacific, 2013. Emerg Infect Dis 20: 1085-1086.

527 3. Johansson MA, Mier-y-Teran-Romero L, Reefhuis J, Gilboa SM, Hills SL (2016) Zika and the
528 Risk of Microcephaly. N Engl J Med 375: 1-4.

529 4. Liu Y, Liu J, Du S, Shan C, Nie K, et al. (2017) Evolutionary enhancement of Zika virus
530 infectivity in Aedes aegypti mosquitoes. Nature 545: 482-486.

531 5. Yuan L, Huang XY, Liu ZY, Zhang F, Zhu XL, et al. (2017) A single mutation in the prM protein
532 of Zika virus contributes to fetal microcephaly. Science 358: 933-936.

533 6. Rossi SL, Ebel GD, Shan C, Shi PY, Vasilakis N (2018) Did Zika Virus Mutate to Cause Severe
534 Outbreaks? Trends Microbiol 26: 877-885.

535 7. Ferraris P, Yssel H, Misse D (2019) Zika virus infection: an update. Microbes Infect.

536 8. Pierson TC, Diamond MS (2018) The emergence of Zika virus and its new clinical syndromes.
537 Nature 560: 573-581.

538 9. Triunfol M (2016) Microcephaly in Brazil: confidence builds in Zika connection. Lancet Infect Dis
539 16: 527-528.

540 10. Schuler-Faccini L, Ribeiro EM, Feitosa IM, Horovitz DD, Cavalcanti DP, et al. (2016) Possible
541 Association Between Zika Virus Infection and Microcephaly - Brazil, 2015. MMWR Morb
542 Mortal Wkly Rep 65: 59-62.

543 11. Chimelli L, Melo ASO, Avvad-Portari E, Wiley CA, Camacho AHS, et al. (2017) The spectrum
544 of neuropathological changes associated with congenital Zika virus infection. Acta
545 Neuropathol 133: 983-999.

546 12. Del Campo M, Feitosa IM, Ribeiro EM, Horovitz DD, Pessoa AL, et al. (2017) The phenotypic
547 spectrum of congenital Zika syndrome. Am J Med Genet A 173: 841-857.

548 13. Franca GV, Schuler-Faccini L, Oliveira WK, Henriques CM, Carmo EH, et al. (2016) Congenital
549 Zika virus syndrome in Brazil: a case series of the first 1501 livebirths with complete
550 investigation. Lancet 388: 891-897.

551 14. Wen Z, Song H, Ming GL (2017) How does Zika virus cause microcephaly? Genes Dev 31: 849-
552 861.

553 15. Rasmussen SA, Jamieson DJ, Honein MA, Petersen LR (2016) Zika Virus and Birth Defects--
554 Reviewing the Evidence for Causality. N Engl J Med 374: 1981-1987.

555 16. Mlakar J, Korva M, Tul N, Popovic M, Poljsak-Prijatelj M, et al. (2016) Zika Virus Associated
556 with Microcephaly. N Engl J Med 374: 951-958.

557 17. Morris G, Barichello T, Stubbs B, Kohler CA, Carvalho AF, et al. (2018) Zika Virus as an
558 Emerging Neuropathogen: Mechanisms of Neurovirulence and Neuro-Immune Interactions.
559 Mol Neurobiol 55: 4160-4184.

560 18. Li H, Saucedo-Cuevas L, Shresta S, Gleeson JG (2016) The Neurobiology of Zika Virus. Neuron
561 92: 949-958.

562 19. Miner JJ, Diamond MS (2017) Zika Virus Pathogenesis and Tissue Tropism. Cell Host Microbe
563 21: 134-142.

564 20. Christian KM, Song H, Ming GL (2019) Pathophysiology and Mechanisms of Zika Virus
565 Infection in the Nervous System. Annu Rev Neurosci 42: 249-269.

566 21. Figueiredo CP, Barros-Aragao FGQ, Neris RLS, Frost PS, Soares C, et al. (2019) Zika virus
567 replicates in adult human brain tissue and impairs synapses and memory in mice. Nat
568 Commun 10: 3890.

569 22. Tiwari SK, Dang J, Qin Y, Lichinchi G, Bansal V, et al. (2017) Zika virus infection reprograms
570 global transcription of host cells to allow sustained infection. Emerg Microbes Infect 6: e24.

571 23. Arora N, Sadovsky Y, Dermody TS, Coyne CB (2017) Microbial Vertical Transmission during
572 Human Pregnancy. Cell Host Microbe 21: 561-567.

573 24. Khaiboullina SF, Ribeiro FM, Uppal T, Martynova EV, Rizvanov AA, et al. (2019) Zika Virus
574 Transmission Through Blood Tissue Barriers. Front Microbiol 10: 1465.

575 25. Bayer A, Lennemann NJ, Ouyang Y, Bramley JC, Morosky S, et al. (2016) Type III Interferons
576 Produced by Human Placental Trophoblasts Confer Protection against Zika Virus Infection.
577 Cell Host Microbe 19: 705-712.

578 26. Tabata T, Petitt M, Puerta-Guardo H, Michlmayr D, Wang C, et al. (2016) Zika Virus Targets
579 Different Primary Human Placental Cells, Suggesting Two Routes for Vertical Transmission.
580 Cell Host Microbe 20: 155-166.

581 27. Quicke KM, Bowen JR, Johnson EL, McDonald CE, Ma H, et al. (2016) Zika Virus Infects
582 Human Placental Macrophages. Cell Host Microbe 20: 83-90.

583 28. Aagaard KM, Lahon A, Suter MA, Arya RP, Seferovic MD, et al. (2017) Primary Human
584 Placental Trophoblasts are Permissive for Zika Virus (ZIKV) Replication. Sci Rep 7: 41389.

585 29. Weisblum Y, Oiknine-Djian E, Vorontsov OM, Haimov-Kochman R, Zakay-Rones Z, et al.
586 (2017) Zika Virus Infects Early- and Midgestation Human Maternal Decidual Tissues,
587 Inducing Distinct Innate Tissue Responses in the Maternal-Fetal Interface. J Virol 91:
588 e01905-01916.

589 30. Brasil P, Pereira JP, Jr., Moreira ME, Ribeiro Nogueira RM, Damasceno L, et al. (2016) Zika
590 Virus Infection in Pregnant Women in Rio de Janeiro. N Engl J Med 375: 2321-2334.

591 31. Shapiro-Mendoza CK, Rice ME, Galang RR, Fulton AC, VanMaldeghem K, et al. (2017)
592 Pregnancy Outcomes After Maternal Zika Virus Infection During Pregnancy - U.S.
593 Territories, January 1, 2016-April 25, 2017. MMWR Morb Mortal Wkly Rep 66: 615-621.

594 32. Caires-Junior LC, Goulart E, Melo US, Araujo BHS, Alvizi L, et al. (2018) Discordant congenital
595 Zika syndrome twins show differential in vitro viral susceptibility of neural progenitor cells.
596 Nat Commun 9: 475.

597 33. McGrath EL, Rossi SL, Gao J, Widen SG, Grant AC, et al. (2017) Differential Responses of
598 Human Fetal Brain Neural Stem Cells to Zika Virus Infection. Stem Cell Reports 8: 715-727.

599 34. Amita M, Adachi K, Alexenko AP, Sinha S, Schust DJ, et al. (2013) Complete and unidirectional
600 conversion of human embryonic stem cells to trophoblast by BMP4. Proc Natl Acad Sci U S
601 A 110: E1212-1221.

602 35. Sheridan MA, Yunusov D, Balaraman V, Alexenko AP, Yabe S, et al. (2017) Vulnerability of
603 primitive human placental trophoblast to Zika virus. Proc Natl Acad Sci U S A 114: E1587-
604 E1596.

605 36. Lee CQ, Gardner L, Turco M, Zhao N, Murray MJ, et al. (2016) What Is Trophoblast? A
606 Combination of Criteria Define Human First-Trimester Trophoblast. Stem Cell Reports 6:
607 257-272.

608 37. Roberts RM, Fisher SJ (2011) Trophoblast stem cells. Biol Reprod 84: 412-421.

609 38. Perera-Lecoin M, Meertens L, Carnec X, Amara A (2013) Flavivirus entry receptors: an update.
610 Viruses 6: 69-88.

611 39. Lee I, Bos S, Li G, Wang S, Gadea G, et al. (2018) Probing Molecular Insights into Zika Virus(-
612)Host Interactions. Viruses 10: 233.

613 40. Hamel R, Dejarnac O, Wichit S, Ekchariyawat P, Neyret A, et al. (2015) Biology of Zika Virus
614 Infection in Human Skin Cells. J Virol 89: 8880-8896.

615 41. Nowakowski TJ, Pollen AA, Di Lullo E, Sandoval-Espinosa C, Bershteyn M, et al. (2016)
616 Expression Analysis Highlights AXL as a Candidate Zika Virus Entry Receptor in Neural
617 Stem Cells. Cell Stem Cell 18: 591-596.

618 42. Richard AS, Shim BS, Kwon YC, Zhang R, Otsuka Y, et al. (2017) AXL-dependent infection of
619 human fetal endothelial cells distinguishes Zika virus from other pathogenic flaviviruses. Proc
620 Natl Acad Sci U S A 114: 2024-2029.

621 43. Ojha CR, Rodriguez M, Karuppan MKM, Lapierre J, Kashanchi F, et al. (2019) Toll-like receptor
622 3 regulates Zika virus infection and associated host inflammatory response in primary human
623 astrocytes. PLoS One 14: e0208543.

624 44. Strange DP, Jiyarom B, Pourhabibi Zarandi N, Xie X, Baker C, et al. (2019) Axl Promotes Zika
625 Virus Entry and Modulates the Antiviral State of Human Sertoli Cells. MBio 10.

626 45. Stitt TN, Conn G, Gore M, Lai C, Bruno J, et al. (1995) The anticoagulation factor protein S and
627 its relative, Gas6, are ligands for the Tyro 3/Axl family of receptor tyrosine kinases. Cell 80:
628 661-670.

629 46. Pardy RD, Valbon SF, Richer MJ (2019) Running interference: Interplay between Zika virus and
630 the host interferon response. Cytokine 119: 7-15.

631 47. Caine EA, Scheaffer SM, Arora N, Zaitsev K, Artyomov MN, et al. (2019) Interferon lambda
632 protects the female reproductive tract against Zika virus infection. Nat Commun 10: 280.

633 48. Yockey LJ, Iwasaki A (2018) Interferons and Proinflammatory Cytokines in Pregnancy and Fetal
634 Development. Immunity 49: 397-412.

635 49. Ander SE, Diamond MS, Coyne CB (2019) Immune responses at the maternal-fetal interface. Sci
636 Immunol 4.

637 50. Wu KY, Zuo GL, Li XF, Ye Q, Deng YQ, et al. (2016) Vertical transmission of Zika virus
638 targeting the radial glial cells affects cortex development of offspring mice. Cell Res 26: 645-
639 654.

640 51. Miner JJ, Cao B, Govero J, Smith AM, Fernandez E, et al. (2016) Zika Virus Infection during
641 Pregnancy in Mice Causes Placental Damage and Fetal Demise. Cell 165: 1081-1091.

642 52. Hirsch AJ, Smith JL, Haese NN, Broeckel RM, Parkins CJ, et al. (2017) Zika Virus infection of
643 rhesus macaques leads to viral persistence in multiple tissues. PLoS Pathog 13: e1006219.

644 53. Dudley DM, Aliota MT, Mohr EL, Weiler AM, Lehrer-Brey G, et al. (2016) A rhesus macaque
645 model of Asian-lineage Zika virus infection. Nat Commun 7: 12204.

646 54. Tang H, Hammack C, Ogden SC, Wen Z, Qian X, et al. (2016) Zika Virus Infects Human
647 Cortical Neural Progenitors and Attenuates Their Growth. Cell Stem Cell 18: 587-590.

648 55. Kim JA, Seong RK, Son SW, Shin OS (2019) Insights into ZIKV-Mediated Innate Immune
649 Responses in Human Dermal Fibroblasts and Epidermal Keratinocytes. J Invest Dermatol
650 139: 391-399.

651 56. Lee JK, Shin OS (2019) Advances in Zika Virus(-)Host Cell Interaction: Current Knowledge and
652 Future Perspectives. Int J Mol Sci 20: 1101.

653 57. Counotte MJ, Kim CR, Wang J, Bernstein K, Deal CD, et al. (2018) Sexual transmission of Zika
654 virus and other flaviviruses: A living systematic review. PLoS Med 15: e1002611.

655 58. El Costa H, Gouilly J, Mansuy JM, Chen Q, Levy C, et al. (2016) ZIKA virus reveals broad
656 tissue and cell tropism during the first trimester of pregnancy. Sci Rep 6: 35296.

657 59. Foy BD, Kobylinski KC, Chilson Foy JL, Blitvich BJ, Travassos da Rosa A, et al. (2011)
658 Probable non-vector-borne transmission of Zika virus, Colorado, USA. Emerg Infect Dis 17:
659 880-882.

660 60. D'Ortenzio E, Matheron S, Yazdanpanah Y, de Lamballerie X, Hubert B, et al. (2016) Evidence
661 of Sexual Transmission of Zika Virus. N Engl J Med 374: 2195-2198.

662 61. Calvet G, Aguiar RS, Melo ASO, Sampaio SA, de Filippis I, et al. (2016) Detection and
663 sequencing of Zika virus from amniotic fluid of fetuses with microcephaly in Brazil: a case
664 study. Lancet Infect Dis 16: 653-660.

665 62. Tan L, Lacko LA, Zhou T, Tomoiaga D, Hurtado R, et al. (2019) Pre- and peri-implantation Zika
666 virus infection impairs fetal development by targeting trophectoderm cells. Nat Commun 10:
667 4155.

668 63. Pagani I, Ghezzi S, Ulisse A, Rubio A, Turrini F, et al. (2017) Human Endometrial Stromal Cells
669 Are Highly Permissive To Productive Infection by Zika Virus. Sci Rep 7: 44286.

670 64. Wells AI, Coyne CB (2018) Type III Interferons in Antiviral Defenses at Barrier Surfaces.
671 Trends Immunol 39: 848-858.

672 65. Chen J, Liang Y, Yi P, Xu L, Hawkins HK, et al. (2017) Outcomes of Congenital Zika Disease
673 Depend on Timing of Infection and Maternal-Fetal Interferon Action. Cell Rep 21: 1588-
674 1599.

675 66. Levy JA (2009) The unexpected pleiotropic activities of RANTES. J Immunol 182: 3945-3946.

676 67. Appay V, Rowland-Jones SL (2001) RANTES: a versatile and controversial chemokine. Trends
677 Immunol 22: 83-87.

678 68. Vazirinejad R, Ahmadi Z, Kazemi Arababadi M, Hassanshahi G, Kennedy D (2014) The
679 biological functions, structure and sources of CXCL10 and its outstanding part in the
680 pathophysiology of multiple sclerosis. Neuroimmunomodulation 21: 322-330.

681 69. Arima K, Nasu K, Narahara H, Fujisawa K, Matsui N, et al. (2000) Effects of lipopolysaccharide
682 and cytokines on production of RANTES by cultured human endometrial stromal cells. Mol
683 Hum Reprod 6: 246-251.

684 70. Fujiwara H, Higuchi T, Sato Y, Nishioka Y, Zeng BX, et al. (2005) Regulation of human
685 extravillous trophoblast function by membrane-bound peptidases. Biochim Biophys Acta
686 1751: 26-32.

687 71. Kayisli UA, Mahutte NG, Arici A (2002) Uterine chemokines in reproductive physiology and
688 pathology. Am J Reprod Immunol 47: 213-221.

689 72. Dominguez F, Martinez S, Quinonero A, Loro F, Horcajadas JA, et al. (2008) CXCL10 and IL-6
690 induce chemotaxis in human trophoblast cell lines. Mol Hum Reprod 14: 423-430.

691 73. Cao B, Diamond MS, Mysorekar IU (2017) Maternal-Fetal Transmission of Zika Virus: Routes
692 and Signals for Infection. J Interferon Cytokine Res 37: 287-294.

693 74. Red-Horse K, Zhou Y, Genbacev O, Prakobphol A, Foulk R, et al. (2004) Trophoblast
694 differentiation during embryo implantation and formation of the maternal-fetal interface. J
695 Clin Invest 114: 744-754.

696 75. Kolundzic N, Bojic-Trbojevic Z, Kovacevic T, Stefanoska I, Kadoya T, et al. (2011) Galectin-1 is
697 part of human trophoblast invasion machinery--a functional study in vitro. PLoS One 6:
698 e28514.

699 76. Kolundzic N, Bojic-Trbojevic Z, Radojcic L, Petronijevic M, Vicovac L (2011) Galectin-8 is
700 expressed by villous and extravillous trophoblast of the human placenta. Placenta 32: 909-
701 911.

702 77. He P, Shao D, Ye M, Zhang G (2015) Analysis of gene expression identifies candidate markers
703 and pathways in pre-eclampsia. J Obstet Gynaecol 35: 578-584.

704 78. Vambergue A, Fajardy I (2011) Consequences of gestational and pregestational diabetes on
705 placental function and birth weight. World J Diabetes 2: 196-203.

706 79. Fazleabas AT, Bell SC, Fleming S, Sun J, Lessey BA (1997) Distribution of integrins and the
707 extracellular matrix proteins in the baboon endometrium during the menstrual cycle and early
708 pregnancy. Biol Reprod 56: 348-356.

709 80. Damsky CH, Fitzgerald ML, Fisher SJ (1992) Distribution patterns of extracellular matrix
710 components and adhesion receptors are intricately modulated during first trimester
711 cytotrophoblast differentiation along the invasive pathway, in vivo. J Clin Invest 89: 210-222.

712 81. Zhou Y, Damsky CH, Chiu K, Roberts JM, Fisher SJ (1993) Preeclampsia is associated with
713 abnormal expression of adhesion molecules by invasive cytotrophoblasts. J Clin Invest 91:
714 950-960.

715 82. Kim MS, Yu JH, Lee MY, Kim AL, Jo MH, et al. (2016) Differential Expression of Extracellular
716 Matrix and Adhesion Molecules in Fetal-Origin Amniotic Epithelial Cells of Preeclamptic
717 Pregnancy. PLoS One 11: e0156038.

718 83. Bojic-Trbojevic Z, Jovanovic Krivokuca M, Vilotic A, Kolundzic N, Stefanoska I, et al. (2019)
719 Human trophoblast requires galectin-3 for cell migration and invasion. Sci Rep 9: 2136.

720 84. Hutter S, Knabl J, Andergassen U, Hofmann S, Kuhn C, et al. (2016) Placental Expression
721 Patterns of Galectin-1, Galectin-2, Galectin-3 and Galectin-13 in Cases of Intrauterine
722 Growth Restriction (IUGR). Int J Mol Sci 17: 523.

723 85. Hou PS, Chuang CY, Kao CF, Chou SJ, Stone L, et al. (2013) LHX2 regulates the neural
724 differentiation of human embryonic stem cells via transcriptional modulation of PAX6 and
725 CER1. Nucleic Acids Res 41: 7753-7770.

726 86. Kumamoto T, Hanashima C (2017) Evolutionary conservation and conversion of Foxg1 function
727 in brain development. Dev Growth Differ 59: 258-269.

728 87. Barbier A, Boivin A, Yoon W, Vallerand D, Platt RW, et al. (2013) New reference curves for
729 head circumference at birth, by gestational age. Pediatrics 131: e1158-1167.

730 88. Faria NR, Azevedo R, Kraemer MUG, Souza R, Cunha MS, et al. (2016) Zika virus in the
731 Americas: Early epidemiological and genetic findings. Science 352: 345-349.

732 89. Chen S, Zhou Y, Chen Y, Gu J (2018) fastp: an ultra-fast all-in-one FASTQ preprocessor.
733 Bioinformatics 34: i884-i890.

734 90. Li B, Dewey CN (2011) RSEM: accurate transcript quantification from RNA-Seq data with or
735 without a reference genome. BMC Bioinformatics 12: 323.

736 91. Dobin A, Davis CA, Schlesinger F, Drenkow J, Zaleski C, et al. (2013) STAR: ultrafast universal
737 RNA-seq aligner. Bioinformatics 29: 15-21.

738 92. Frankish A, Diekhans M, Ferreira A-M, Johnson R, Jungreis I, et al. (2018) GENCODE reference
739 annotation for the human and mouse genomes. Nucleic Acids Research 47: D766-D773.

740 93. McCarthy DJ, Chen Y, Smyth GK (2012) Differential expression analysis of multifactor RNA-
741 Seq experiments with respect to biological variation. Nucleic Acids Research 40: 4288-4297.

742 94. Yu G, Wang L-G, Han Y, He Q-Y (2012) clusterProfiler: an R Package for Comparing
743 Biological Themes Among Gene Clusters. OMICS: A Journal of Integrative Biology 16: 284-
744 287.

745
746
747
748
749
750

751 ## Figure captions

752 **Fig 1. Experimental design and ZIKV^{BR} infection in hiPSC-derived trophoblasts.**
753 **(A).** Schematic: generation of trophoblasts from congenital Zika syndrome affected and non-affected
754 discordant twins' hiPSCs followed by ZIKV^{BR} infection and analysis. Silhouettes are courtesy of
755 www.vecteezy.com (mother) and Yulia Ryabokon (babies). (**B).** Immunofluorescence for (β-CG,
756 human chorionic gonadotropin β) and KRT7 (CK7, cytokeratin 7, a pan trophoblast marker) in
757 hiPSC-derived trophoblasts. Scale bar: 20 μm. (**C).** ZIKV PFU/mL in trophoblasts' supernatant at
758 MOI = 0.3 and MOI = 3; mean ± SEM of the three twins; *$p < 0.05$; Student's t test. (**D).**
759 Representative plaque forming assay wells with stained VERO cells exposed to ZIKV collected at 96
760 hpi from the culture supernatants of affected or non-affected #10608 twins' hiPSC-derived
761 trophoblasts infected at a MOI of 0.3.
762

763 **Fig 2. Gene expression analyses of RNA-Seq data from hiPSC-derived trophoblasts from non-**
764 **affected and CZS-affected twins in culture after ZIKV^{BR} infection.**
765 **(A).** Heatmap representation and clusterization of differentially expressed genes (DEGs) (FDR <
766 0.05; edgeR exact test), one in each line, in trophoblasts in culture after ZIKV^{BR} infection (purple bar
767 at top) compared with control non-infected trophoblasts (blue bar at top), in cells derived from both
768 non-affected (#10608-4, #10763-4, and #10788-4) and CZS-affected (#10608-1, #10763-1, and
769 #10788-1) twins (one in each column, as indicated at the bottom). Color scale bar at right = Z score.
770 (**B).** Gene Ontology terms enrichment analysis of upregulated genes in hiPSC-derived trophoblasts
771 after ZIKV^{BR} *in vitro* infection. The three major GO term categories, namely Biological Process,
772 Cellular Component and Molecular Function are separately represented in each panel. The size of the
773 circles is proportional to the number of genes in each significantly enriched category, as indicated at
774 the lower part scales; the colors show the statistical significance of the enrichment, as indicated by
775 the -log10 FDR values that appear in the color-coded scales at the bottom. A GO enrichment
776 significance cutoff of FDR ≤ 0.05 was used.
777
778 **Fig 3. Interferon responses in hiPSC-derived trophoblast after ZIKV^{BR} infection.**
779 **(A).** Pathway enrichment of genes detected as differentially expressed (FDR < 0.05) between hiPSC-
780 derived trophoblasts from non-affected and CZS-affected twins at 96 h after ZIKV^{BR} *in vitro*
781 infection; analysis was carried out with the ingenuity pathway analysis (IPA) tool. Gene upregulation
782 is depicted in shades of red, from white (not significantly changed), to dark red (highly upregulated).
783 **(B).** Luminex quantitation of IFNA, IFNG and IFNL1 detected in the supernatants of hiPSC-derived
784 trophoblasts in culture, from non-affected or CZS-affected twins at 48 h or 96 h after ZIKV^{BR}
785 infection. Data are represented as mean ± SEM and p-value * < 0.05 (Paired Student's t test).
786
787 **Fig 4. Differential gene expression between hiPSC-derived trophoblast from CZS-affected and**
788 **non-affected twins after ZIKV^{BR} infection.**
789 **(A).** Heatmap representation and clusterization of differentially expressed genes (DEGs) (FDR <
790 0.05; edgeR exact test), one in each line, after ZIKV^{BR} *in vitro* infection of trophoblasts from non-
791 affected twins (green bar at top; #10608-4, #10763-4, and #10788-4) as compared with trophoblasts
792 from CZS-affected twins (pink bar at top; #10608-1, #10763-1, and #10788-1) (one in each column,
793 as indicated at the bottom). Color scale bar at right = Z score. (**B).** Gene Ontology terms enrichment
794 analysis of downregulated genes in hiPSC-derived trophoblasts from CZS-affected twins when
795 compared with trophoblasts from non-affected twins after ZIKV^{BR} *in vitro* infection. The three major
796 GO term categories, namely Biological Process, Cellular Component and Molecular Function are
797 separately represented in each panel. The size of the circles is proportional to the number of genes in
798 each significantly enriched category, as indicated at the scales in the lower part; the colors show the
799 statistical significance of the enrichment, as indicated by the -log10 FDR values that appear in the
800 color-coded scales at the bottom. A GO enrichment significance cutoff of FDR ≤ 0.05 was used. **C.**
801 Luminex quantitation of RANTES/CCL5 and IP10 detected in the culture supernatants of hiPSC-
802 derived trophoblasts from non-affected twins or from CZS-affected twins at 48 h (left panels) or 96 h
803 (right panels) after ZIKV^{BR} infection. Data are represented as mean ± SEM and p-value * < 0.05
804 (Paired Student's t test).

805 ## Supporting information

806

807 **S1 Fig**. **Expression measured by RT-qPCR of marker genes of hiPSCs and trophoblasts**.
808 Expression measured by RT-qPCR of *NANOG*, a hiPSC marker, and of *HCGA*, *HCGB* and *KRT7*,
809 three of the genes upregulated in the trophoblasts as compared with the hiPSCs. Twins from each
810 family are represented with a different color: red, #10608 twins; blue, #10763 twins; green, #10788
811 twins. (mean ± SEM; n = 2 biological replicates, except for #10763 due to sample loss during
812 culture)

813 **S2 Fig. Expression levels measured by RNA-Seq of proliferation-related genes in the hiPSCs**
814 **and in the hiPSC-derived trophoblasts from non-affected or CZS-affected twins. Related to**
815 **Figure 2.** The bars represent expression levels (in TPM) of selected genes associated with cellular
816 proliferation in hiPSCs from non-affected (light blue, hiPSC NA) or CZS-affected (dark blue, hiPSC
817 Aff) twins, in the hiPSC-derived trophoblasts from non-affected twins' mock (yellow, Troph – NA-
818 Mock) or ZIKV-infected cells (orange, Troph – NA-MOI 0.3), and in the hiPSC-derived trophoblasts
819 from CZS-affected twins' mock (red, Troph – Aff-Mock) or ZIKV-infected cells (brown, Troph –
820 Aff-MOI 0.3). The levels of expression of the genes were compared between non-affected (both non-
821 infected and infected) trophoblasts and non-affected hiPSCs; and from CZS-affected (both non-
822 infected and infected) trophoblasts and CZS-affected hiPSCs. Genes significantly down-regulated in
823 trophoblast cells when compared with hiPSCs are shown (one-away ANOVA, p-value threshold was
824 * 0.05, ** 0.01, *** 0.001 and **** 0.0001). Error bars show SEM.

825 **S3 Fig. Expression levels measured by RNA-Seq of genes encoding candidate attachment**
826 **factors implicated in ZIKV infection of human cells. Related to Figure 2.** The bars represent
827 expression levels (in TPM) of eight candidate ZIKV attachment factor genes in hiPSCs from non-
828 affected (light blue, hiPSC NA) or CZS-affected (dark blue, hiPSC Aff) twins, in the hiPSC-derived
829 trophoblasts from non-affected twins' mock (yellow, Troph – NA-Mock) or ZIKV-infected cells
830 (orange, Troph – NA-MOI 0.3), and in the hiPSC-derived trophoblasts from CZS-affected twins'
831 mock (red, Troph – Aff-Mock) or ZIKV-infected cells (brown, Troph – Aff-MOI 0.3). None of these
832 genes was significantly differentially expressed in hiPSC-derived trophoblasts from CZS-affected
833 twins, when compared with hiPSC-derived trophoblasts from non-affected twins in pairwise
834 comparisons (two-tailed t-test, equal variance). Error bars show SEM.

835 **S4 Fig. Expression levels measured by RNA-Seq of genes encoding representatives of Type I,**
836 **Type II, and Type III IFNs. Related to Figure 2.** The bars represent expression levels (in TPM) of
837 genes encoding interferons in hiPSCs from non-affected (light blue, hiPSC NA) or CZS-affected
838 (dark blue, hiPSC Aff) twins, in the hiPSC-derived trophoblasts from non-affected twins' mock
839 (yellow, Troph – NA-Mock) or ZIKV-infected cells (orange, Troph – NA-MOI 0.3), and in the
840 hiPSC-derived trophoblasts from CZS-affected twins' mock (red, Troph – Aff-Mock) or ZIVK-
841 infected cells (brown, Troph – Aff-MOI 0.3). None of these genes was significantly differentially
842 expressed in hiPSC-derived trophoblasts from CZS-affected twins when compared with hiPSC-
843 derived trophoblasts from non-affected twins in pairwise comparisons (two-tailed t-test, equal
844 variance). None of the 13 recognized human *IFNA* (*IFNA1, 2, 4, 5, 6, 7, 8, 10, 13, 14, 16, 17, 21*),

845 *IFNG*, *IFNK* and *IFNW1* genes were significantly expressed in any of the data sets. Error bars show
846 SEM.

847 **S5 Fig. Expression levels measured by RNA-Seq of genes encoding receptors for Type I, Type**
848 **II, and Type III IFNs. Related to Figure 2**. The bars represent expression levels (in TPM) of genes
849 encoding interferon receptors in hiPSCs from non-affected (light blue, hiPSC NA) or CZS-affected
850 (dark blue, hiPSC Aff) twins, in the hiPSC-derived trophoblasts from non-affected twins' mock
851 (yellow, Troph – NA-Mock) or ZIKV-infected cells (orange, Troph – NA-MOI 0.3), and in the
852 hiPSC-derived trophoblasts from CZS-affected twins' mock (red, Troph – Aff-Mock) or ZIKV-
853 infected cells (brown, Troph – Aff-MOI 0.3). None of these genes was significantly differentially
854 expressed in hiPSC-derived trophoblasts from CZS-affected twins when compared with hiPSC-
855 derived trophoblasts from non-affected twins in pairwise comparisons (two-tailed t-test, equal
856 variance). Error bars show SEM.

857 **S6 Fig. Differential gene expression between hiPSC-derived trophoblast from CZS-affected and**
858 **non-affected twins after ZIKV^{BR} infection. Related to Figure 4.** Gene Ontology terms enrichment
859 analysis of upregulated genes in hiPSC-derived trophoblasts from CZS-affected compared with non-
860 affected twins after ZIKV^{BR} *in vitro* infection. The major GO term categories, namely Biological
861 Process and Molecular Function are separately represented in each panel. The size of the circles is
862 proportional to the number of genes in each significantly enriched category, as indicated at the lower
863 part scales; the colors show the statistical significance of the enrichment, as indicated by the -log10
864 FDR values that appear in the color-coded scales at the bottom. A GO enrichment significance cutoff
865 of FDR $\leq$ 0.05 was used.

866 **S7 Fig. Expression measured by RT-qPCR of genes found in the RNA-Seq analysis**
867 **downregulated after ZIKV^{BR} infection in trophoblasts from CZS-affected when compared with**
868 **non-affected twins**. Expression measured by RT-qPCR of *COL3A1*, *ITGA1* and *LGALS3*, three of
869 the genes downregulated after ZIKV^{BR} infection in trophoblasts from CZS-affected (Aff) when
870 compared with non-affected (NA) twins. Twins from each family are represented with a different
871 color: red, #10608 twins; blue, #10763 twins; green, #10788 twins. Mean ± SEM is shown. (n = 2
872 biological replicates, except for #10763 due to sample loss during culture; One-tailed t-test, *
873 $p<0.05$).

874

875 **Fig 1**

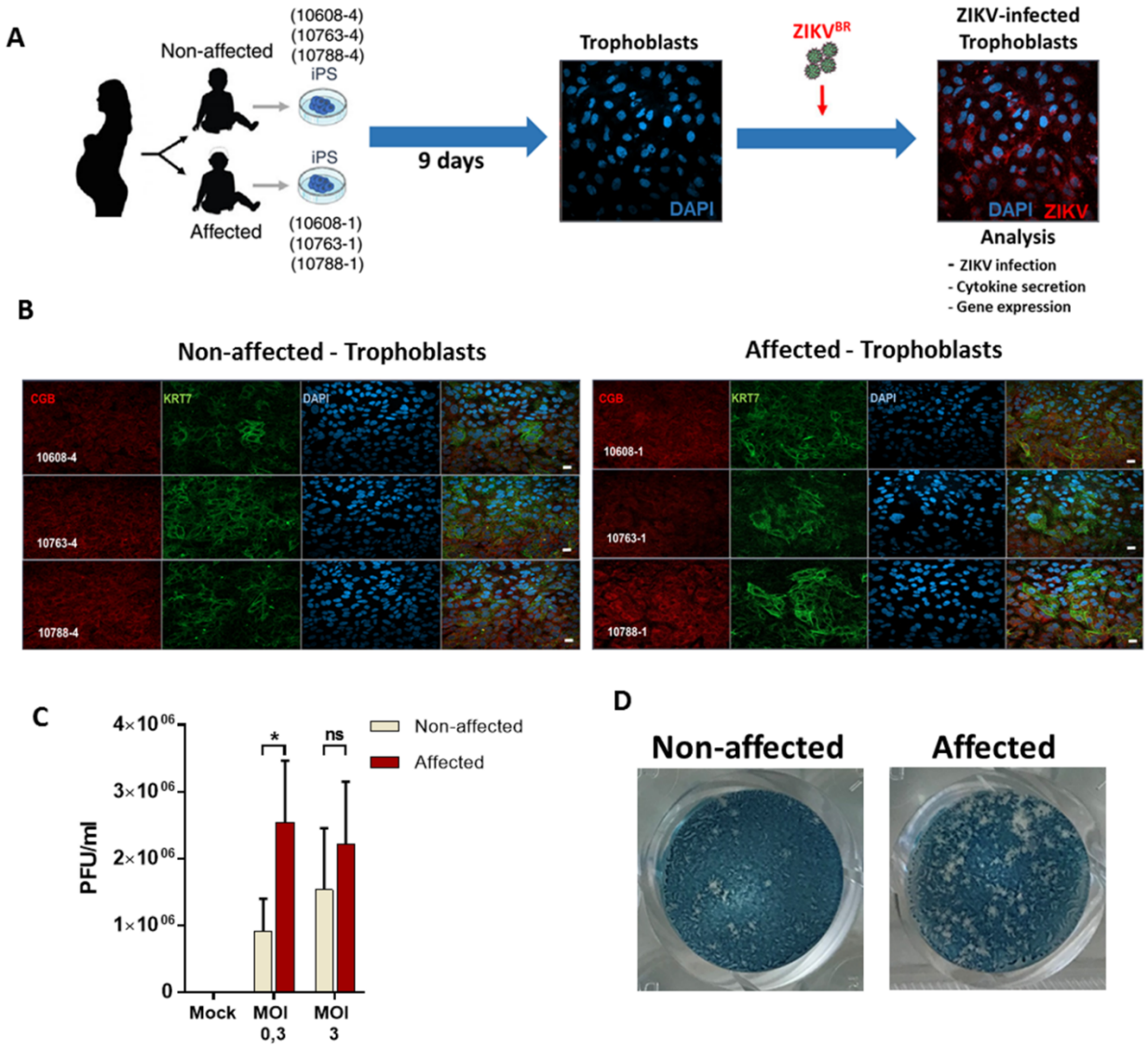

876

877

878

879

880 **Fig 2**

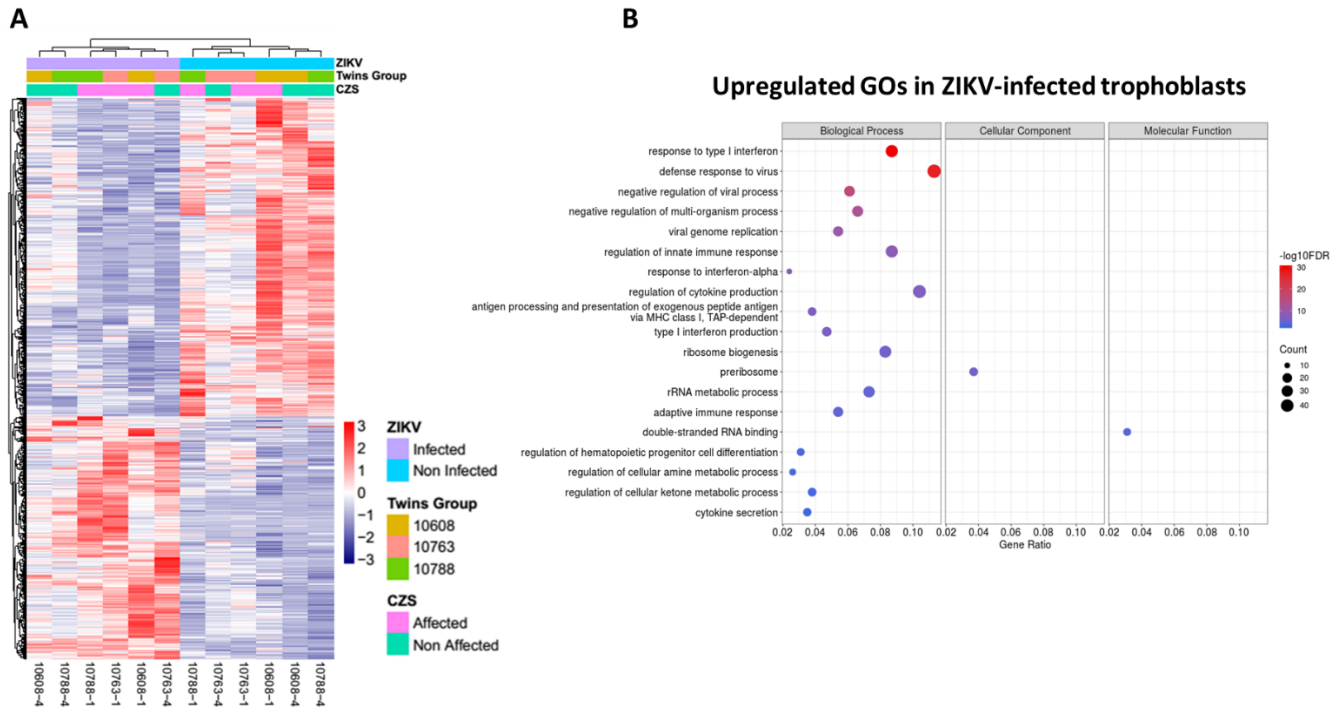

881

882

883

884

885 **Fig 3**

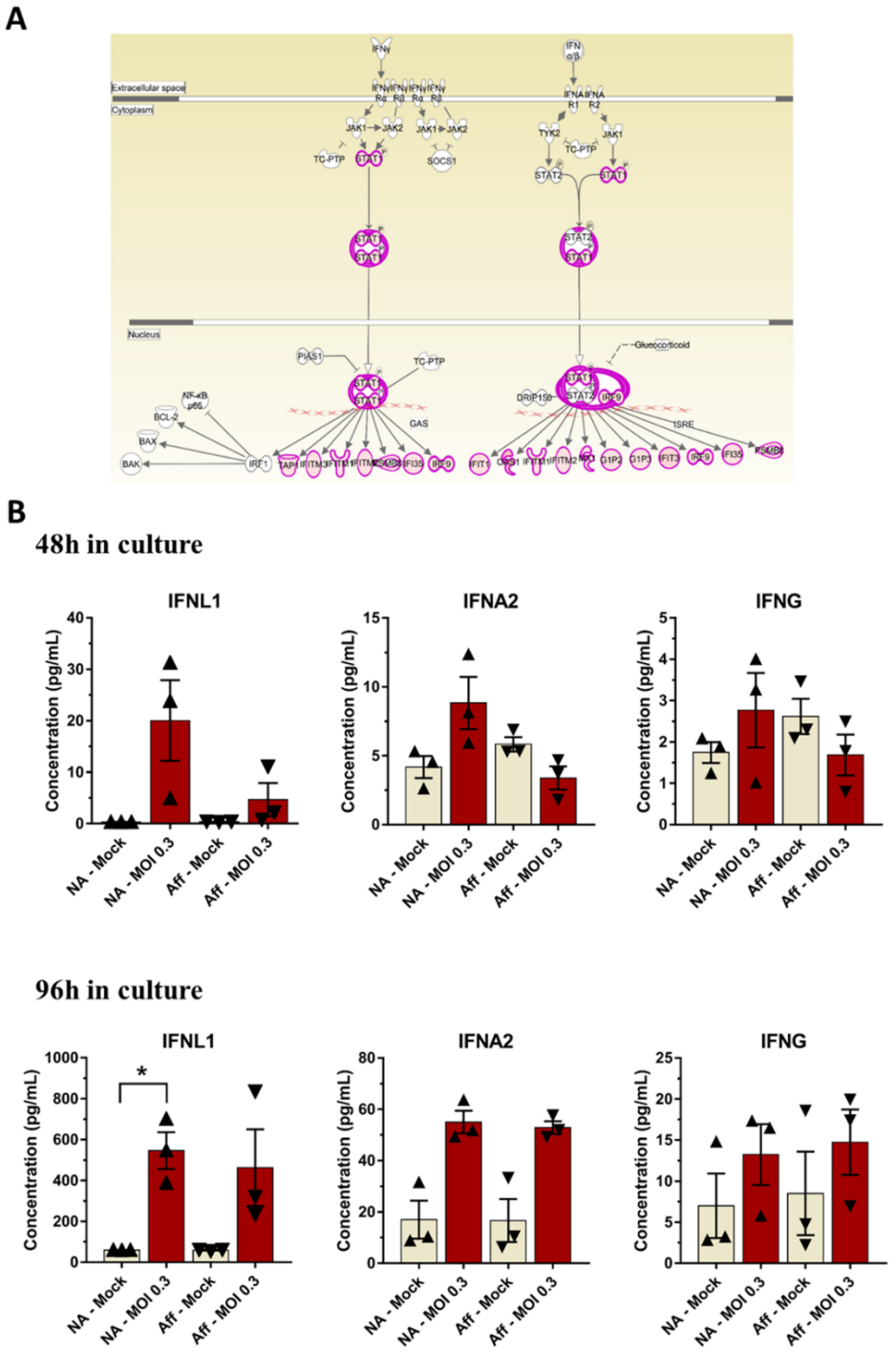

886

887

888

Fig 4

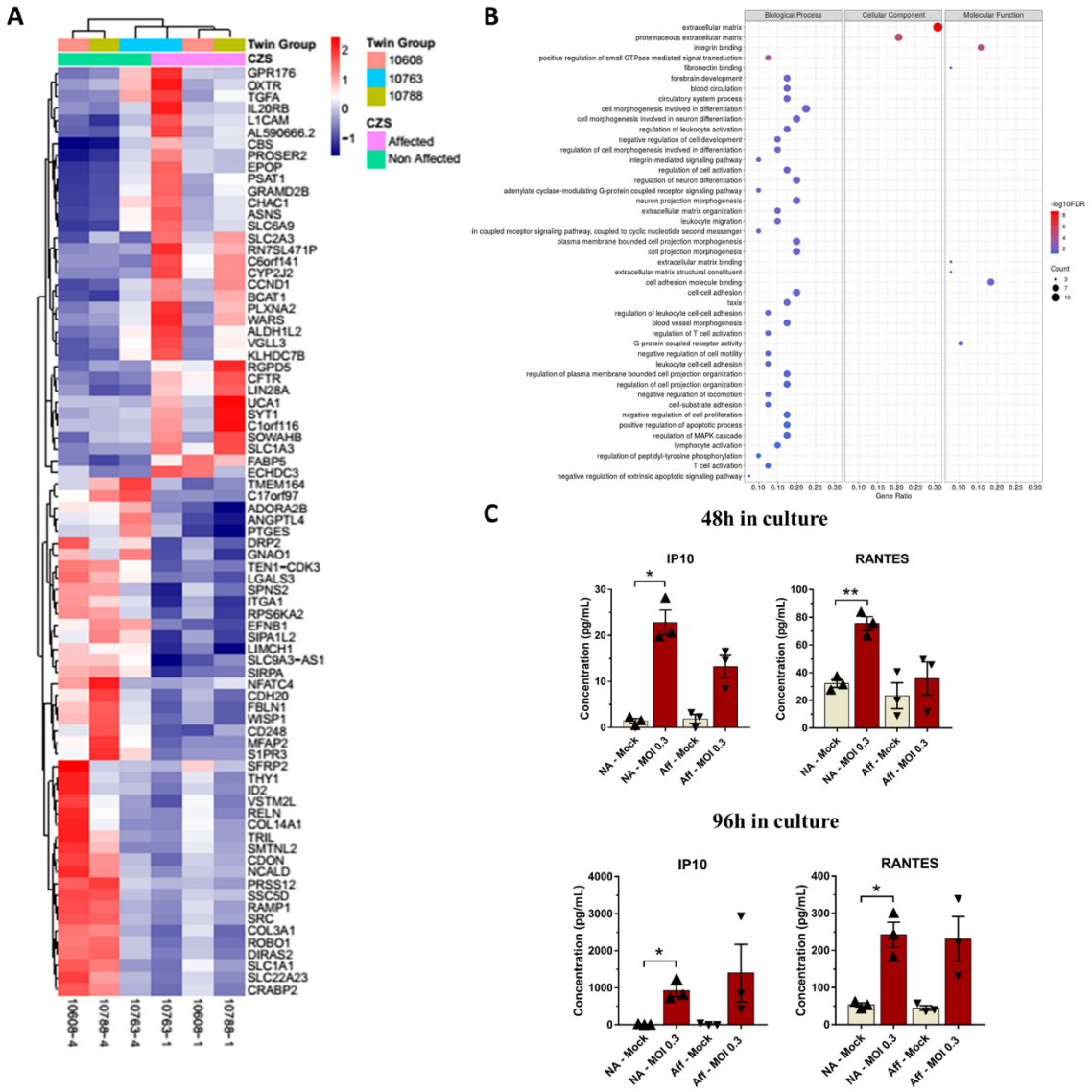
A
Twin Group
CZS
Twin Group
10608
10763
10788
CZS
Affected
Non Affected
GPR176
OXTR
TGFA
IL20RB
L1CAM
AL590666.2
CBS
PROSER2
EPOP
PSAT1
GRAMD2B
CHAC1
ASNS
SLC6A9
SLC2A3
RN7SL471P
C6orf141
CYP2J2
CCND1
BCAT1
PLXNA2
WARS
ALDH1L2
VGLL3
KLHDC7B
RGPD5
CFTR
LIN28A
UCA1
SYT1
C1orf116
SOWAHB
SLC1A3
FABP5
ECHDC3
TMEM164
C17orf97
ADORA2B
ANGPTL4
PTGES
DRP2
GNAO1
TEN1-CDK3
LGALS3
SPNS2
ITGA1
RPS6KA2
EFNB1
SIPA1L2
LIMCH1
SLC9A3-AS1
SIRPA
NFATC4
CDH20
FBLN1
WISP1
CD248
MFAP2
S1PR3
SFRP2
THY1
ID2
VSTM2L
RELN
COL14A1
TRIL
SMTNL2
CDON
NCALD
PRSS12
SSC5D
RAMP1
SRC
COL3A1
ROBO1
DIRAS2
SLC1A1
SLC22A23
CRABP2
10608-4
10788-4
10763-4
10763-1
10608-1
10788-1
B
Biological Process
Cellular Component
Molecular Function
extracellular matrix
proteinaceous extracellular matrix
integrin binding
positive regulation of small GTPase mediated signal transduction
fibronectin binding
forebrain development
blood circulation
circulatory system process
cell morphogenesis involved in differentiation
cell morphogenesis involved in neuron differentiation
regulation of leukocyte activation
negative regulation of cell development
regulation of cell morphogenesis involved in differentiation
integrin-mediated signaling pathway
regulation of cell activation
regulation of neuron differentiation
adenylate cyclase-modulating G-protein coupled receptor signaling pathway
neuron projection morphogenesis
extracellular matrix organization
leukocyte migration
in coupled receptor signaling pathway, coupled to cyclic nucleotide second messenger
plasma membrane bounded cell projection morphogenesis
cell projection morphogenesis
extracellular matrix binding
extracellular matrix structural constituent
cell adhesion molecule binding
cell-cell adhesion
taxis
regulation of leukocyte cell-cell adhesion
blood vessel morphogenesis
regulation of T cell activation
G-protein coupled receptor activity
negative regulation of cell motility
leukocyte cell-cell adhesion
regulation of plasma membrane bounded cell projection organization
regulation of cell projection organization
negative regulation of locomotion
cell-substrate adhesion
negative regulation of cell proliferation
positive regulation of apoptotic process
regulation of MAPK cascade
lymphocyte activation
regulation of peptidyl-tyrosine phosphorylation
T cell activation
negative regulation of extrinsic apoptotic signaling pathway
Gene Ratio
-log10FDR
Count
C
48h in culture
IP10
RANTES
Concentration (pg/mL)
NA - Mock
NA - MOI 0.3
Aff - Mock
Aff - MOI 0.3
96h in culture
IP10
RANTES
Concentration (pg/mL)
NA - Mock
NA - MOI 0.3
Aff - Mock
Aff - MOI 0.3

Supporting information

S1 Fig

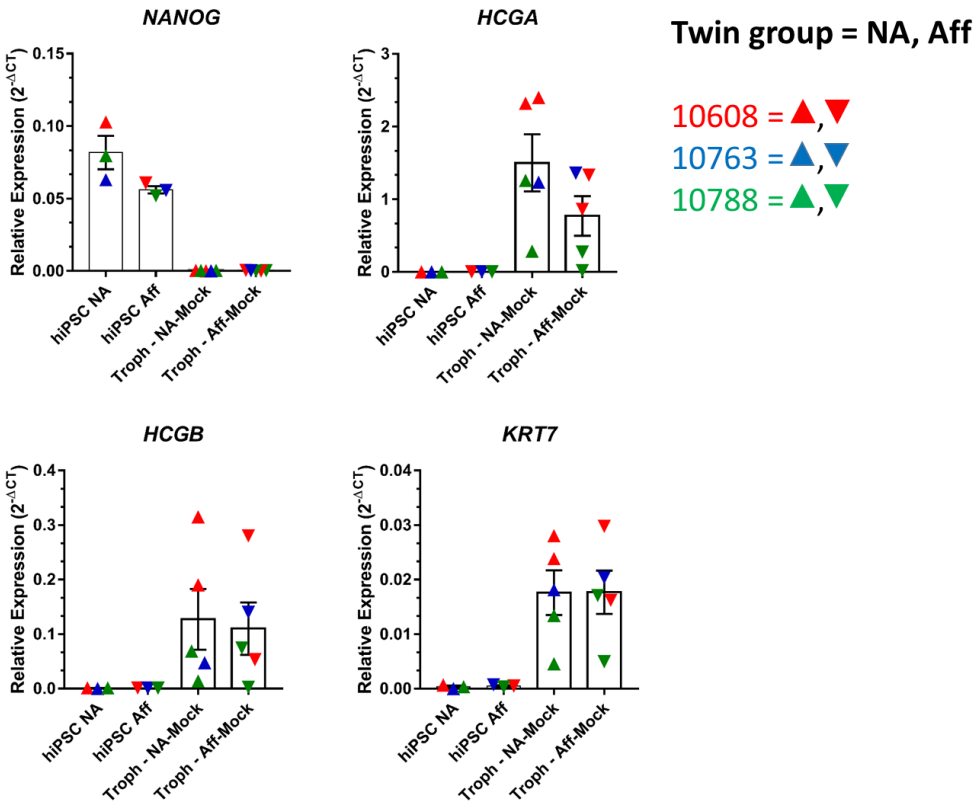

898 **S2 Fig**

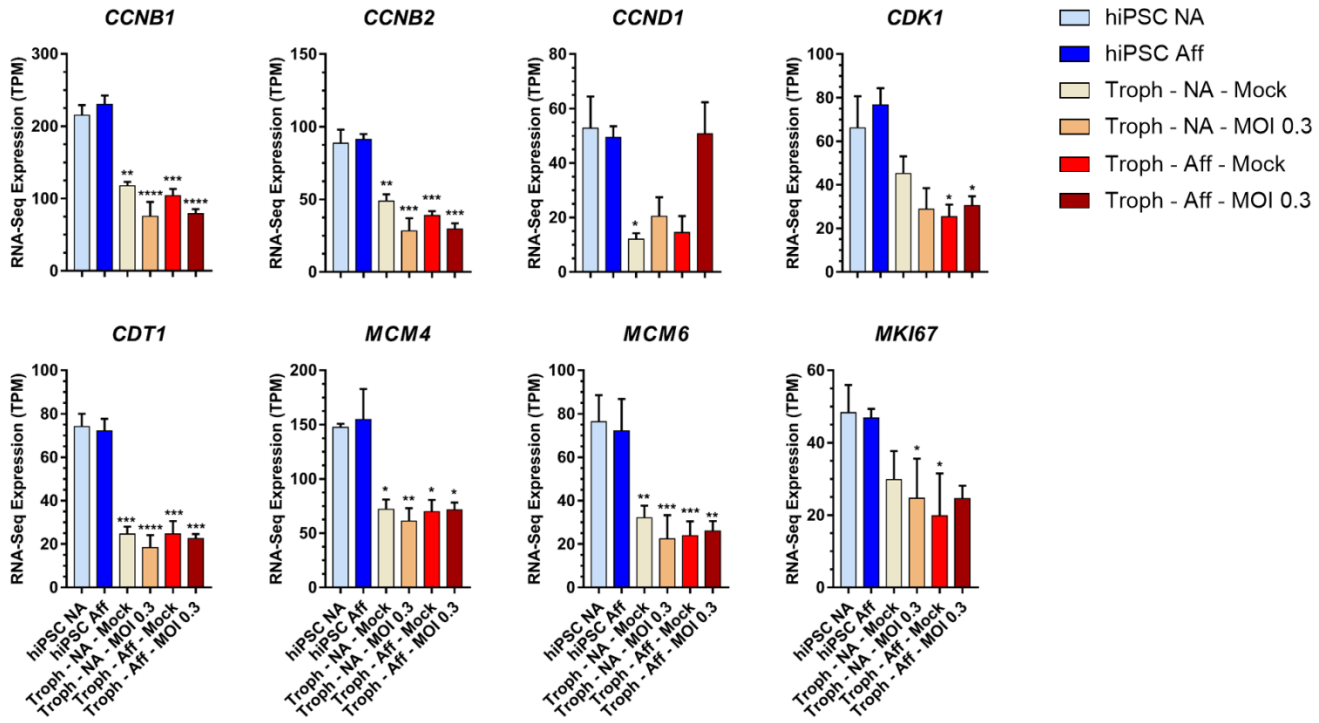

899

900

901

902

903 **S3 Fig**

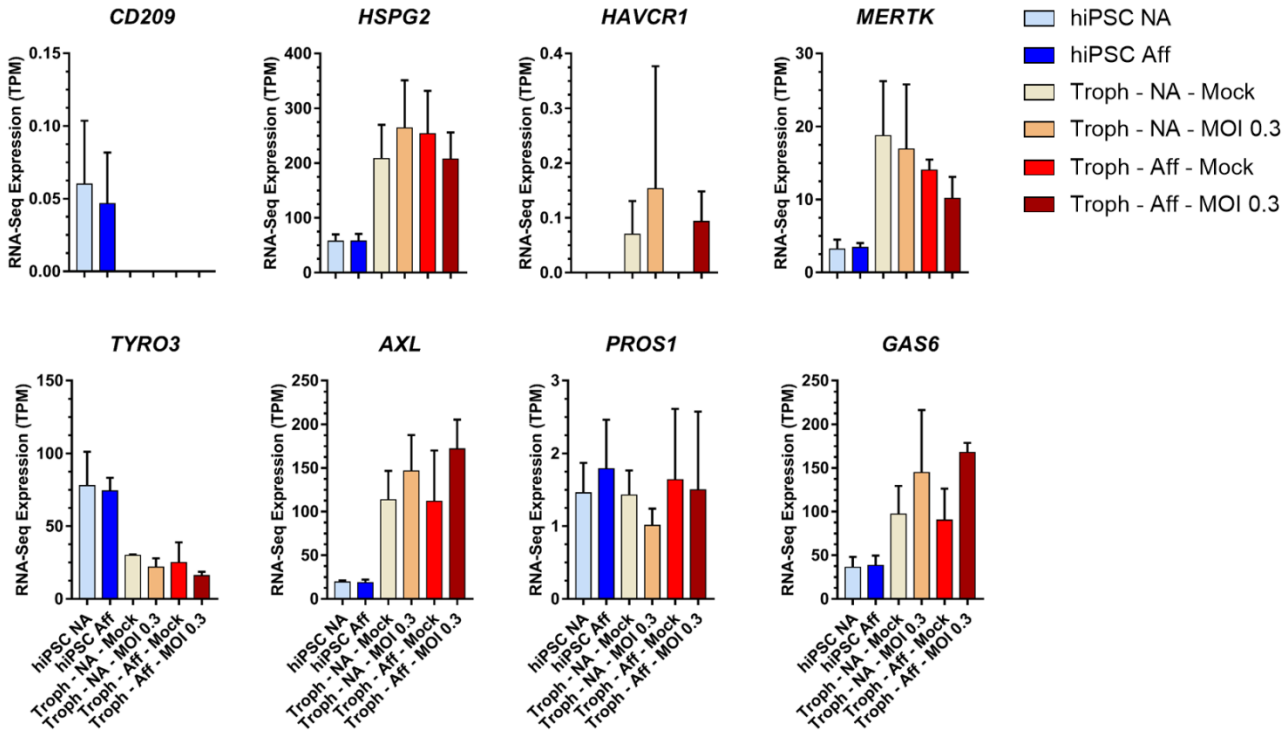

904

905

906

907 **S4 Fig**

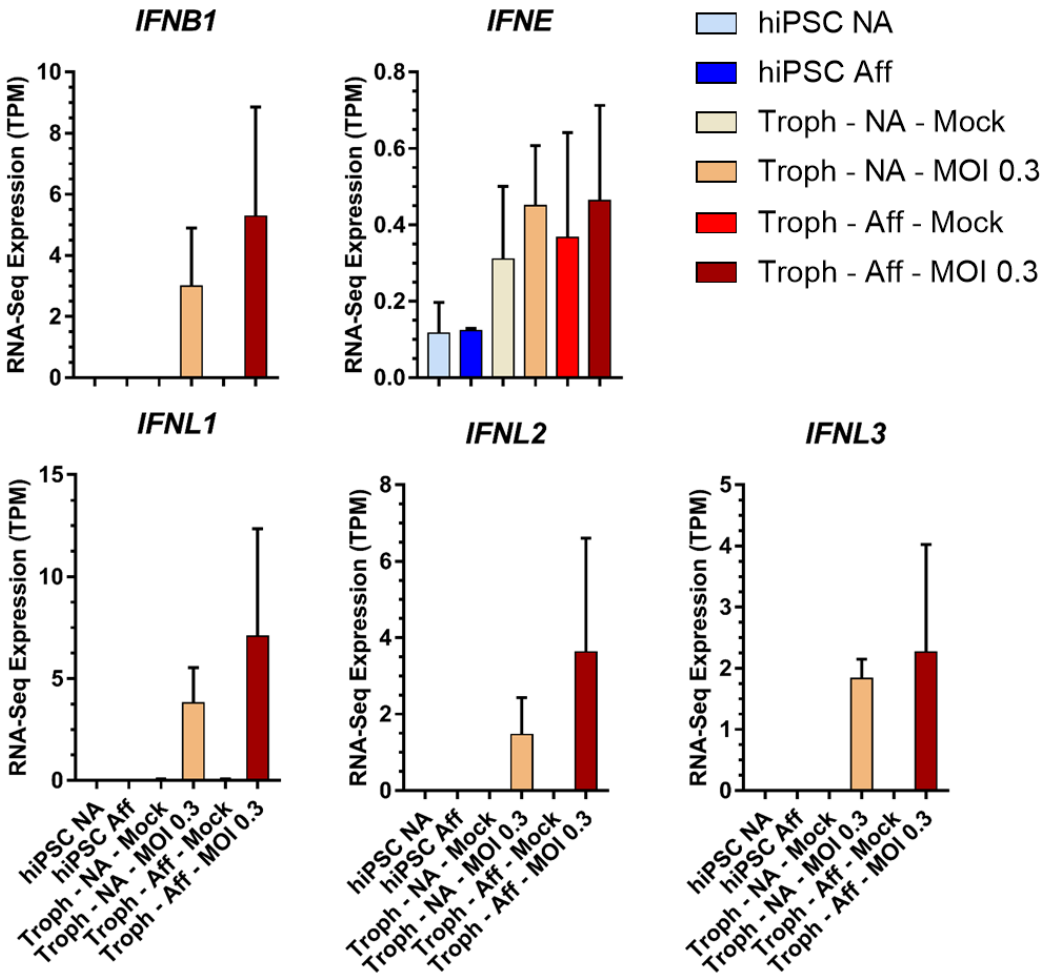

908

909

910

911 **S5 Fig**

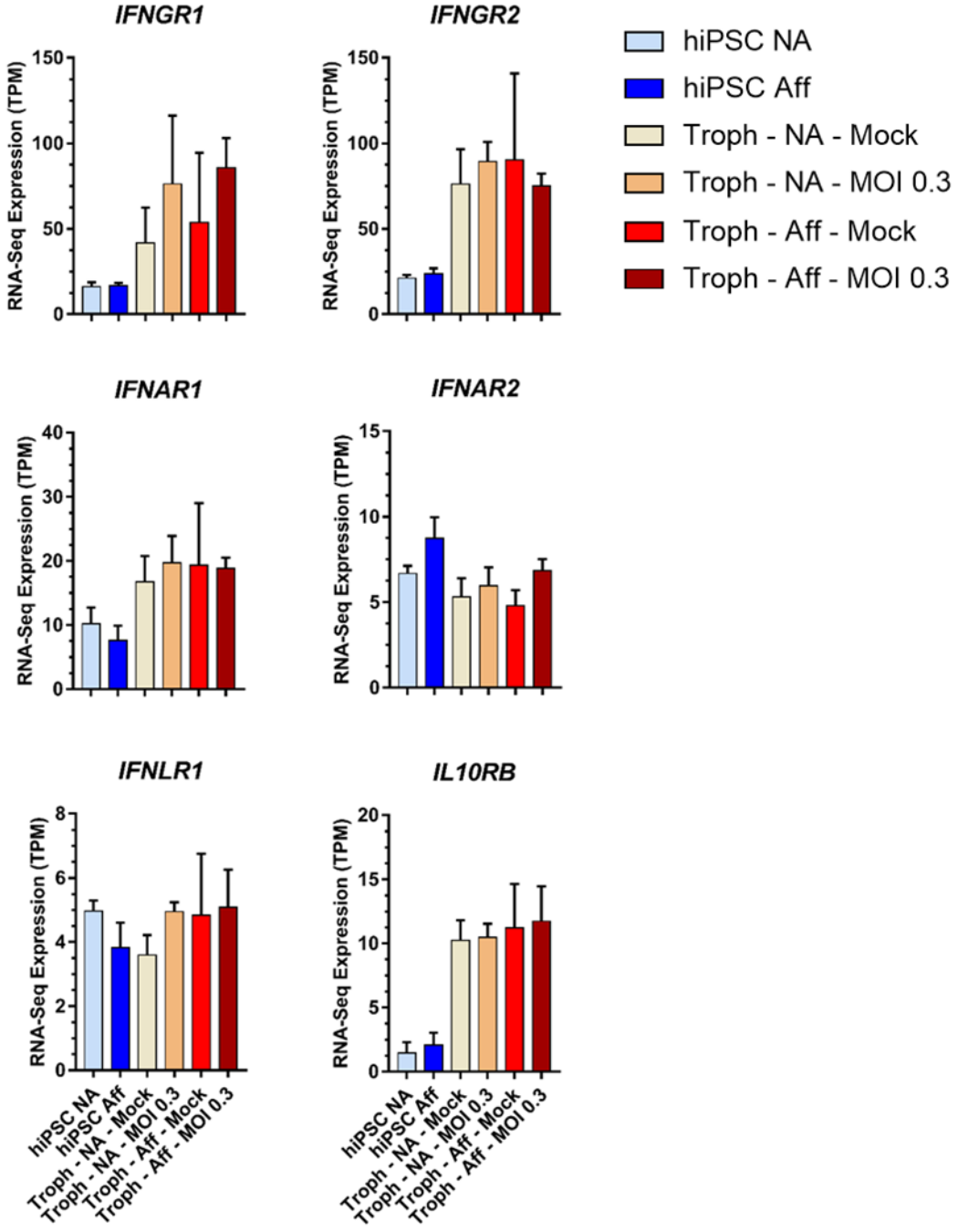

912

913

914 **S6 Fig**

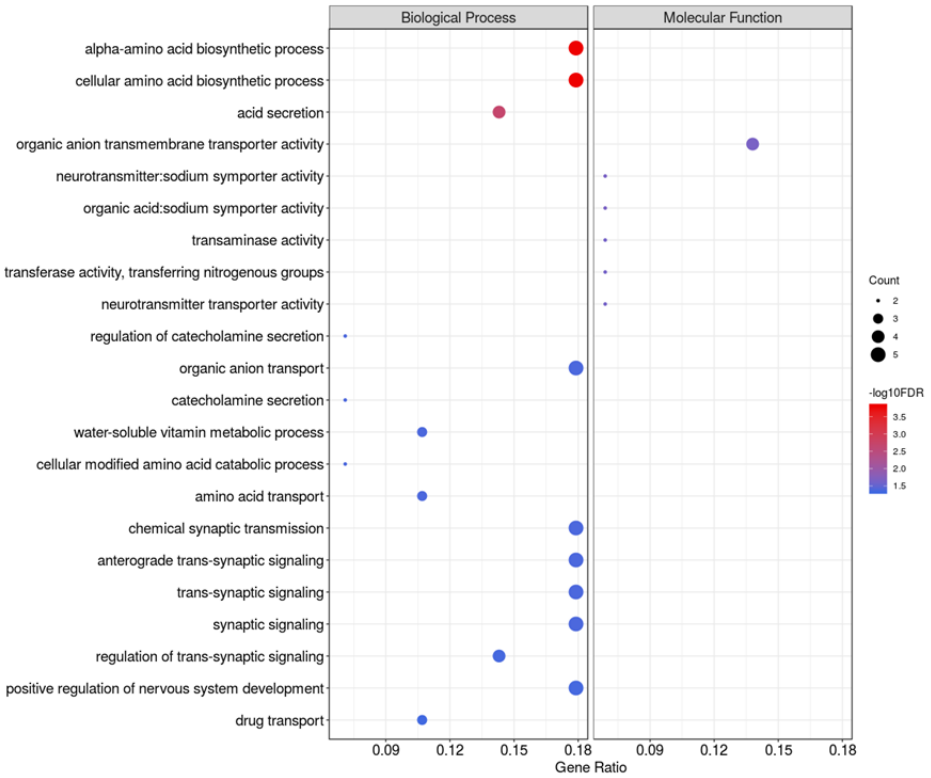

915

916

917

918

S7 Fig

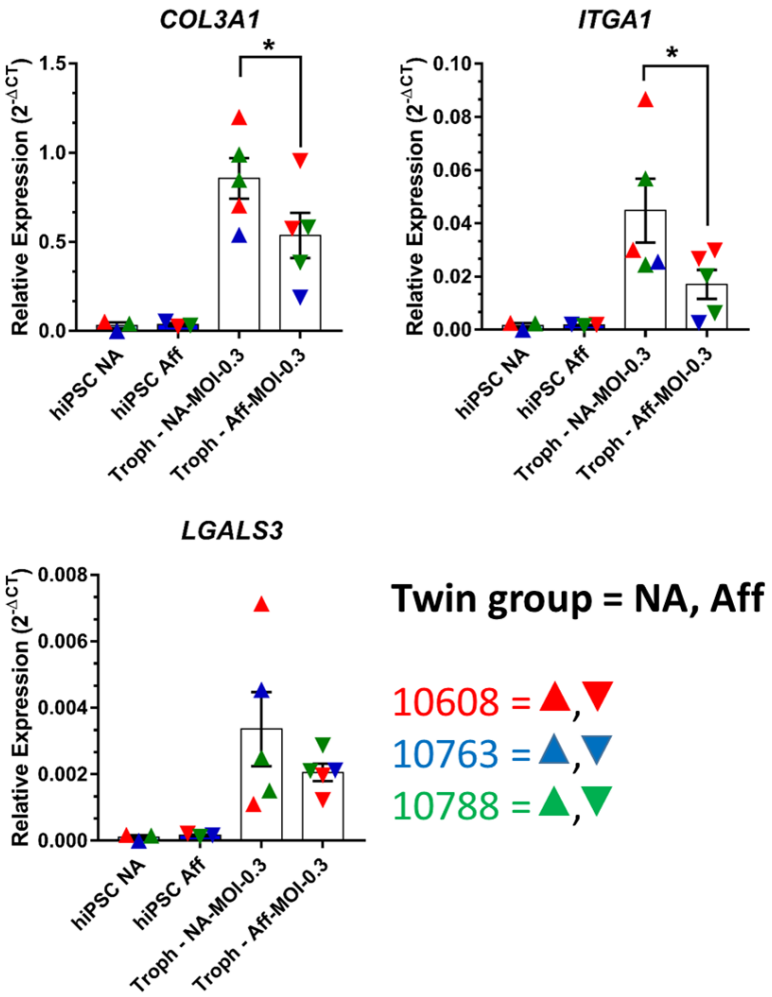
COL3A1
ITGA1
LGALS3
Relative Expression (2^-ΔCT)
hiPSC NA
hiPSC Aff
Troph - NA-MOI-0.3
Troph - Aff-MOI-0.3
*
Twin group = NA, Aff
10608 = ▲,▼
10763 = ▲,▼
10788 = ▲,▼